frontiers | Frontiers in Nanotechnology

TYPE Original Research
PUBLISHED 20 May 2025
DOI 10.3389/fnano.2025.1569453

OPEN ACCESS

EDITED BY
Ramesh Namdeo Pudake,
Amity University, India

REVIEWED BY
Binod Bihari Sahu,
National Institute of Technology Rourkela, India
Hugo Gerardo Lazcano-Ramirez,
Autonomous University of Zacatecas, Mexico

*CORRESPONDENCE
Besma Sghaier-Hammami,
besma.sghaier@inat.ucar.tn
Sofiene B. M. Hammami,
sofiene.hammami@inat.ucar.tn

†These authors have contributed equally to this work

RECEIVED 31 January 2025
ACCEPTED 10 April 2025
PUBLISHED 20 May 2025

CITATION
Belhedi M, Sghaier-Hammami B, Masiello M, Nafati H, Somma S, Gambacorta L, Salhi R, Messaoud M, Labidi S, Moretti A and Hammami SBM (2025) Silicon dioxide (SiO_2) nanoparticles affect the morphology, sporulation, mycotoxin production, and pathogenicity of *Fusarium brachygibbosum* infecting olive trees.
Front. Nanotechnol. 7:1569453.
doi: 10.3389/fnano.2025.1569453

Silicon dioxide (SiO_2) nanoparticles affect the morphology, sporulation, mycotoxin production, and pathogenicity of *Fusarium brachygibbosum* infecting olive trees

Meryam Belhedi[1,2†], Besma Sghaier-Hammami[2*†], Mario Masiello[3], Haythem Nafati[4], Stefania Somma[3], Lucia Gambacorta[3], Rached Salhi[5,6], Mouna Messaoud[6], Sonia Labidi[1], Antonio Moretti[3] and Sofiene B. M. Hammami[1*]

[1]Horticultural Sciences Laboratory, LR13AGR01, National Agronomic Institute of Tunisia, University of Carthage, Tunis, Tunisia, [2]Laboratory of Bioggressors and Integrated Pest Management in Agriculture, LR14AGR02, National Agronomic Institute of Tunisia, University of Carthage Tunis, Tunis, Tunisia, [3]Institute of Sciences of Food Production, National Research Council, Bari, Italy, [4]Faculté des Sciences de Tunis, Département Physique, Tunis, Tunisia, [5]GMP, IUT 1, University Grenoble Alpes, Grenoble, France, [6]Laboratory of Advanced Materials, National School of Engineers of Sfax, University of Sfax, Sfax, Tunisia

Introduction: This study investigates the *In Vitro* antifungal activity of silicon dioxide nanoparticles (SiO_2 NPs) against mycotoxigenic *Fusarium brachygibbosum* species, a fungus posing a significant threat to olive trees in Tunisia.

Methods: Two different doses of SiO_2 NPs (100 and 200 mg kg^{-1}) were used to evaluate its effect on fungal growth, mycotoxin production, and virulence capability of tested *F. brachygibbosum* strain.

Results and Discussion: While mycelial growth was not influenced by SiO_2 NPs, a notable increase in macroconidia sporulation was observed at the highest dose tested. Scanning electron microscopy revealed structural alterations in fungal hyphae treated with SiO_2 NPs, including hyphal disorganization after the adherence of nanoparticles. Furthermore, SiO_2 NPs influenced oxidative stress in *Fusarium*, with varying effects on hydrogen peroxide levels, total antioxidant activity, and total phenolic compounds, modulating the capability of the fungus to produce mycotoxins. Indeed, fusaric acid and 15-acetyldeoxynivalenol amounts decreased in presence of SiO_2, while an increasing level of neosolaniol and diacetoxyscirpenol was observed. Pathogenicity tests on olive and sorghum leaves revealed a reduction of disease severity in SiO_2 treated samples compared to untreated controls, showcasing the potential of SiO_2 NPs as a sustainable alternative for managing *Fusarium* infections. These findings underline the potential use of SiO_2 NPs as environmentally friendly and effective tool in integrated pest management strategies against *F. brachygibbosum* as well as other *Fusarium* species

occurring on olive trees. Further research is warranted to optimize their application and understand their interactions with both the pathogen and the host plant.

KEYWORDS

***Fusarium spp.*, *Olea europaea*, silicon dioxide nanoparticles, sporulation, mycotoxins, pathogenicity test**

Highlights

- *Fusarium brachygibbosum,* an emerging olive tree pathogen in Tunisia, poses a significant threat to agriculture and requires innovative management solutions.
- Silicon dioxide nanoparticles (SiO_2 NPs) were tested for their effects on *Fusarium*, marking the first such study in Tunisia.
- While SiO_2 NPs did not inhibit mycelial growth, they induced pigmentation and significantly increased macroconidia sporulation at the highest concentrations (200 ppm).
- SiO_2 NPs induced an oxidative stress and a loss of membrane integrity in *F. brachygibbosum.*
- SiO_2 NPs influenced mycotoxin production in *F. brachygibbosum* reducing trichothecenes production
- SiO_2 NPs reduced *Fusarium* pathogenic effects on olive and sorghum leaves, showing promise as an alternative to chemical fungicides.

1 Introduction

Fusarium species are among the most significant phytopathogenic and mycotoxigenic fungi worldwide, causing severe diseases on various economically important crops (Munkvold et al., 2021). Although traditionally associated with major losses in cereals and vegetables, *Fusarium* infections are increasingly reported in olive trees showing symptoms of dieback in several countries worldwide (Nicoletti et al., 2020), including Morocco (Chliyeh et al., 2017), Spain (Hernández et al., 1998), Greece (Markakis et al., 2021), and Tunisia (Gharbi et al., 2020; Trabelsi et al., 2017).

This rise can be attributed to changes in olive cultivation methods, the expansion of new plantations into *Fusarium*-infected areas, and the use of infected planting material. Although *Fusarium* wilt has not yet reached the severity observed with other pathogens such as *Verticillium* species, *Xylella fastidiosa*, *Pseudocercospora*, and *Venturia oleaginea*, studies suggest that it has the potential to become more aggressive, similar to its impact on cereals and vegetables (Verma et al., 2024; Al-Hashimi et al., 2025).

Numerous agronomic strategies, including resistant varieties, chemical treatments, and crop rotation have been proposed to control *Fusarium*. Among these strategies, treatment with synthetic fungicides is the most effective tool against phytopathogenic *Fusarium* species. However, the repeated use of chemicals with the same mode of action could lead to a strong selection of resistant strains (Liu et al., 2019a; Yin et al., 2009; Yuan and Zhou, 2005), making the management of fungal diseases more difficult. Moreover, integrated pest management guidelines and environmental sustainability policies encourage researchers to develop newer eco-friendly strategies to control both fungal species and their mycotoxin accumulation, to reduce chemical treatments and, consequently, their negative environmental impact.

Recently, the new technologies and new knowledge on nanoparticles have encouraged researchers to develop effective nanoparticle-based bio-stimulants and pesticide more eco-friendly than chemical compounds (Duhan et al., 2017; Bhagat et al., 2023; Kumari et al., 2023). In addition, the nanoparticle based products allow the precise release of necessary and sufficient amounts of active ingredients and thus minimal residual presence, and release in the environment (Santosh P. and Yojana S., 2022). Notably, a reduced graphene oxide–copper oxide nanocomposite demonstrated superior antifungal activity at a significantly lower concentration (1 mg/L) compared to a conventional fungicide (2.5 g/L) in controlling *Fusarium* diseases in tomato and pepper plants (El-Abeid et al., 2020), highlighting the potential of nanotechnology in plant protection.

Within this framework, silicon, known as second most abundant element on earth after oxygen (Shahzad et al., 2022), was stated to have an important role in mitigating different stresses occurred on plants (Coskun et al., 2016; Elsheery et al., 2020). Especially its nanosized form which has shown promising results due to its good physical properties than bulk material (Siddiqui et al., 2014). Used as a pesticide, silica nanoparticles have shown potential in controlling various pests such as insects (Ziaee and Ganji, 2016). Moreover, studies who focused on the impact of silicon NPs on the interaction plant-pathogen have demonstrated the capability of silica nanoparticles in stimulating plant's defense mechanisms and controlling phytopathogenic microorganisms (Baazaoui et al., 2021; Bathoova et al., 2021; Hassan et al., 2022; Parveen and Siddiqui, 2022). For instance, Yobo et al. (2019) reported that granular and foliar potassium silicate had a positive effect in controlling Fusarium Head Blight disease of wheat. Likewise, Sakr, (2021a) and Sakr & Shoaib, (2021) demonstrated that treatment of 1.50 g kg^{-1} of soil and 1.7 mM soluble silicon reduced Fusarium Head Blight disease of wheat and barley. Previous studies suggest that SiO_2 NPs may affect fungal cells by disrupting membrane integrity through their accumulation on the cell wall. This accumulation can interfere with the transmembrane energy cycle, disrupt the electron transport chain, and compromise the overall structural integrity of the fungal cells (Derbalah et al., 2018; Abdelrhim et al., 2021). While SiO_2 NPs are reported to have antifungal properties, the underlying molecular mechanisms remain poorly understood.

This study aims to evaluate the *in vitro* antifungal potential activity of silicon dioxide nanoparticles (SiO_2 NPs) against *F. brachygibbosum*, an emerging pathogen threatening Tunisian

olive trees and recognized as a potential Union quarantine pest (Bragard et al., 2021). This research pioneers the use of SiO_2 NPs as a novel strategy to control *F. brachygibbosum*, offering a promising tool to managing this emerging olive tree pathogen.

2 Material and methods

2.1 Nanoparticle synthesis

The synthesis of SiO_2 nanoparticles was carried out using the sol-gel process combined with supercritical ethanol drying. The preparation began with a solution containing tetraethyl orthosilicate (TEOS), ethanol, and distilled water, as described by Martínez et al. (2006). This mixture was stirred for 30 min to form a transparent sol. Subsequently, hydrofluoric acid (HF) was added gradually to the sol. The resulting mixture was subjected to supercritical drying to produce an aerogel. This step involved placing the sol in an ethanol-filled autoclave, which was heated to 243 °C and pressurized above ethanol's critical point (Tc = 243 °C, Pc = 63 bar). Gelation occurred after maintaining the sol at this temperature for 1 h. The interstitial solvent was removed through a controlled depressurization process over 1 h using nitrogen gas. To prevent thermal strain and cracking, the autoclave was kept sealed for 24 h, allowing thermal equilibrium before it was gradually opened. The characteristic of the obtained SiO_2 aerogel was thoroughly detailed by Sghaier-Hammami et al. (2024).

2.2 Fungal isolation and identification

An orchard in the Kairouan region, located in southwestern Tunisia (35,67°N; 10,10°E), a major area for olive cultivation, was inspected for the presence of olive trees showing dieback symptoms on the aerial parts. A representative sample of olive roots was collected and carried to the laboratory for further analysis. For fungal isolation, root portions were thoroughly rinsed under running tap water for 15 min to remove soil and debris, dried on filter paper, and surface-sterilized using 2% (v/v) sodium hypochlorite for 2 min. They were then rinsed three times for 1 min with sterile distilled water and dried again on sterile filter paper. Small pieces from the margin of symptomatic tissues were transferred on Potato Dextrose Agar (PDA) medium amended with 100 mg L^{-1} streptomycin sulfate and 50 mg L^{-1} neomycin. Petri dishes were incubated at 25 °C for 7 days under an alternating light/darkness cycle of 12 h photoperiod.

After incubation, colonies developed from root pieces were transferred on new PDA plates and then purified by using the single spore isolation technique. All monosporic strains identified as *Fusarium* were transferred on PDA and Spezieller Nahrstoffarmer agar (SNA) media and morphologically identified according to Leslie & Summerell (2006). Morphological identification of each strain was also confirmed by sequencing the translation elongation factor 1-α gene by using the primer pair EF1/EF2 (O'Donnell et al., 1998), according to the procedure reported by Abi Saad et al. (2022).

2.3 Treatment of *Fusarium brachygibbosum* strain with nanoparticles

In order to test the effect of the SiO_2 NPs on fungal growth of *F. brachygibbosum* species, two different doses were used (100 and 200 ppm). In detail, SiO_2 NPs was added to PDA cooled down to 45°C–50°C after autoclaving and stirred for 10 min on a magnetic stirrer to ensure its homogeneous dispersion in the medium.

To evaluate the effect on fungal growth, *F. brachygibbosum* strain, MB1 stored in ITEM collection (Agro-Food Microbial Culture Collection, ISPA-CNR Bari, Italy, http://server.ispa.cnr.it/ITEM/Collection/) was used for mycelial growth assay. Briefly, mycelium disks (4 mm in diameter) from actively growing margins of 3–5-day old colonies cultured on PDA, were used to inoculate Petri dishes (90 mm in diameter) containing PDA or PDA amended with SiO_2 NPs. The inhibition activity of the SiO_2 NPs on colony growth was determined by measuring the diameter (in mm) of developing colonies after 3, 5, 7, and 10 days of incubation at 25°C, under darkness. The number and size of macroconidia and chlamydospores were also assessed after 7 and 14 days of incubation, respectively. The experiment was conducted with five replicates per treatment, and the trial was repeated twice.

2.4 *In vitro* pathogenicity test on detached olive leaves and stems, and shoots sorghum

The *In vitro* pathogenicity test on detached olive leaves was performed as described by Liu et al. (2007). To test the virulence of MB1 *F. brachygibbosum* strain treated with SiO_2, olive leaves and stems from the Chemlali cultivar, and leaves of sorghum were collected and injected with conidial suspension. The conidial suspension was prepared by carefully scraping the fungal culture from the amended medium, ensuring that no sterile distilled water was added to the surface to prevent any potential influence of SiO_2 NPs on the leaves.

Samples were collected at the same foliar stage and had approximately the same dimensions. For each treatment, six samples were placed in rectangular Petri dishes on soaked paper moistened with sterilized distilled water. For the control treatment, distilled water was injected into the samples, using the same number of replicates as for the other treatments. An aliquot of 10 µL of conidial suspension (10^6 spore mL^{-1}) or distilled water was injected into the center of each leaf to ensure uniform conditions for all replicates.

2.5 SEM observations

For the morphological and chemical analysis of the fusarium samples, a Thermo Scientific™ Quanta™ 250 FEI scanning electron microscope (SEM), equipped with an Energy-Dispersive X-ray Spectroscopy (EDX) system, was used. This microscope is manufactured by Thermo Fisher Scientific Inc., located in Waltham, Massachusetts, USA.

The SEM provides high-resolution imaging of the sample surfaces at scales ranging from micrometers to nanometers. It uses an electron beam that interacts with the material, generating

signals that are converted into images representing the surface topography. The integrated EDX system enables detailed chemical analysis by detecting and quantifying the elements present in the samples based on the X-ray emissions generated during electron beam interaction. This technique allowed for the identification of chemical elements and the mapping of their distribution within the samples.

Analyses were performed under low vacuum conditions to preserve the integrity of biological and non-conductive samples. Images were obtained at various magnifications to examine surface structures and elemental characteristics. Measurements were carried out in low-voltage mode to reduce the risk of damage to sensitive samples and to enhance electron penetration depth in the materials. The spatial resolution provided by this instrument allowed for the examination of fine surface details, and EDX analysis enabled the determination of the chemical composition at micro- and nanoscale levels.

2.6 Image analysis

Infected zone rate was calculated using the software Image Plus (Motic, version 2.0, 2008) using the formula:

$$\text{Infected zone rate}\,(\%) = \frac{\text{Infected leaf surface}}{\text{Leaf surface}} \times 100$$

For each leaf, the surface area of visible symptoms (necrotic or chlorotic spots) was measured and compared to the total leaf surface

Additionally, hyphal deformation severity was assessed by measuring the mycelium diameter in SEM images using ImageJ software (National Institutes of Health, Bethesda, MD, United States).

2.7 Cell membrane integrity

The integrity of the cell membrane of *F. brachygibbosum* was assessed by UV-VIS spectrophotometry following the method described by Ribeiro et al. (2024), with modifications. Specifically, a sporal suspension of the three treatments, adjusted to approximately 10^6 spore mL^{-1}, was prepared in sterilized distilled water and incubated at 37°C for 2 h. After incubation, the samples were centrifuged, and the supernatant was collected for analysis. The absorbance of the supernatant was measured at 260 nm and 280 nm using a UV-VIS spectrophotometer (UV Spectrophotometer OPTIZEN 3220UV, Daejeon, South Korea).

2.8 Non-enzymatic antioxidant parameters measurements

The total antioxidant activity was measured following the method described by Koleva et al. (2002). Results were expressed in milligrams of gallic acid equivalents per Gram of dry weight (mg GAE/g DW), as outlined in the same study. The calibration curve was constructed within a concentration range of 0–500 μg mL^{-1}.

The total phenolic content of different species was assessed using a modified version of the Folin-Ciocalteu method as described by Pereira et al. (2018). Phenolic content was expressed as milligrams of gallic acid equivalents per Gram of dry residue (mg GAE/g DR), calculated from a calibration curve prepared with gallic acid standards in the range from 0.001 to 0.01 mg L^{-1}.

Hydrogen peroxide (H_2O_2) content in fungi was determined using a modified method based on Velikova et al. (2000). Fungi were rapidly frozen in liquid nitrogen and ground in 5 mL of 0.1% (w/v) trichloroacetic acid. The homogenate was centrifuged at 15,000 × g for 15 min at 4 °C to separate the supernatant. An aliquot of 0.5 mL of the supernatant was combined with 1 mL of 1 M KI and 0.5 mL of 10 mM K_2HPO_4 buffer (pH 7.0). The reaction mixture was kept in darkness for 60 min before measuring absorbance at 390 nm. The H_2O_2 concentration was calculated using a standard curve prepared beforehand.

2.9 Mycotoxins analysis

The effect of SiO_2 NPs, at two different concentrations 100 and 200 mg kg^{-1}, on mycotoxin production was evaluated culturing *F. brachygibbosum* MB1 strain on PDA and PDA amended with the compound. After 14 days of incubation at 25 °C in darkness, mycelial plugs (2 g) were collected in 50 mL tubes containing 10 mL acetonitrile/water/acetic acid (79:20:1, v/v/v). Mycotoxin extraction was obtained by 3 min of slurried. Extracts were diluted in water (ratio 1:10) and directly injected into the LC- HRMS instrument. Liquid chromatography–HMRS analysis was performed on Orbitrap ExplorisTM 240 E, equipped with a heated electrospray ion source (HESI II) coupled to a Vanquish UHPLC system (all from Thermo Fisher Scientific, San Jose, CA, United States). Chromatographic separation was performed at 40 °C on a Gemini® C_{18}-column, 150 × 2 mm i. d., 5 μm particle size, equipped with a C_{18} 4 × 3 mm i. d. security guard cartridge (Phenomenex, Torrance, CA, United States). The flow rate of the mobile phase was 350 μL/min, whereas the injection volume was 10 μL. Eluent A was water, and eluent B was methanol, both containing 0.5% acetic acid and 1 mM ammonium acetate. The HESI II ion source was operated in positive ion mode and in negative mode, with the following settings: sheath gas: 30 arbitrary units, auxiliary gas: five arbitrary units, sweep gas 1 arbitrary units, spray voltage: 3.5 kV for positive ion and 2,5 KV for negative ion, RF lens: 70 percentage (arbitrary units), ion transfer tube: 325°C, vaporizer temperature: 300°C. High-resolution mass spectrometry chromatograms were acquired in positive and negative ionization mod in the same run. Resolution was 120,000 and the scan range (m/z): 70-850. Mycotoxin identification was carried out by comparing retention times, fragmentation patterns, and collision cross-sections with reference standards compiled in our in-house UNIFI library. This library was built by analyzing a mixture of mycotoxin standards under the same analytical conditions.

2.10 Statistical analysis

All data are presented as means. Tukey's HSD test was performed using one-way analysis of variance (ANOVA) by IBM SPSS software (Version 27.0. Armonk, NY: IBM Corp, United States) with a value of $P < 0.05$ being considered significant. Principal component and Pearson's correlation analysis was executed utilizing the FactoMineR packages within the R software, version 4.2.3, with data normalized by applying Z-score standardization prior to PCA.

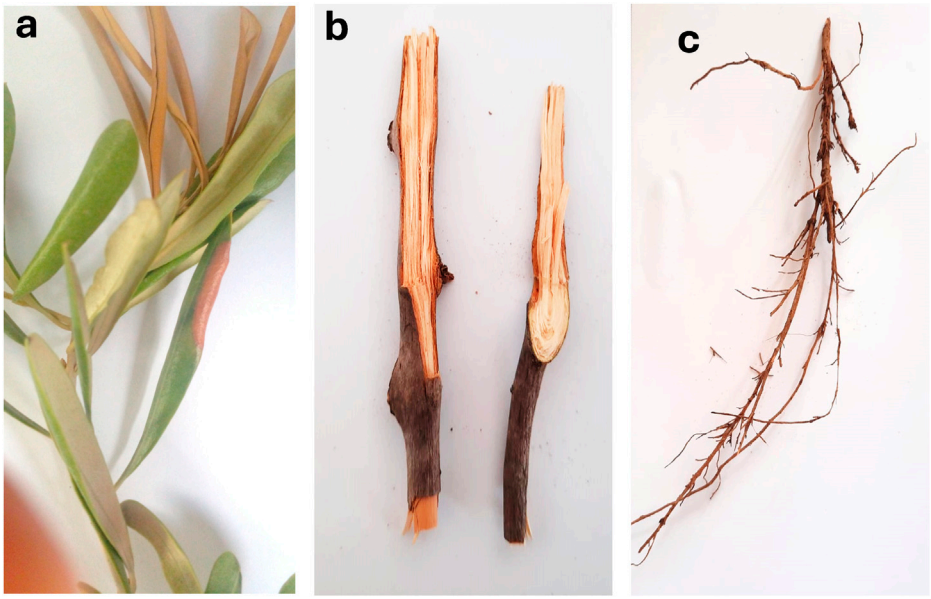

FIGURE 1
Symptoms of *Fusarium* infection on olive trees: **(a)** wilted olive leaves with discoloration, **(b)** internal vascular browning in infected branches, **(c)** root damage and decay caused by the pathogen.

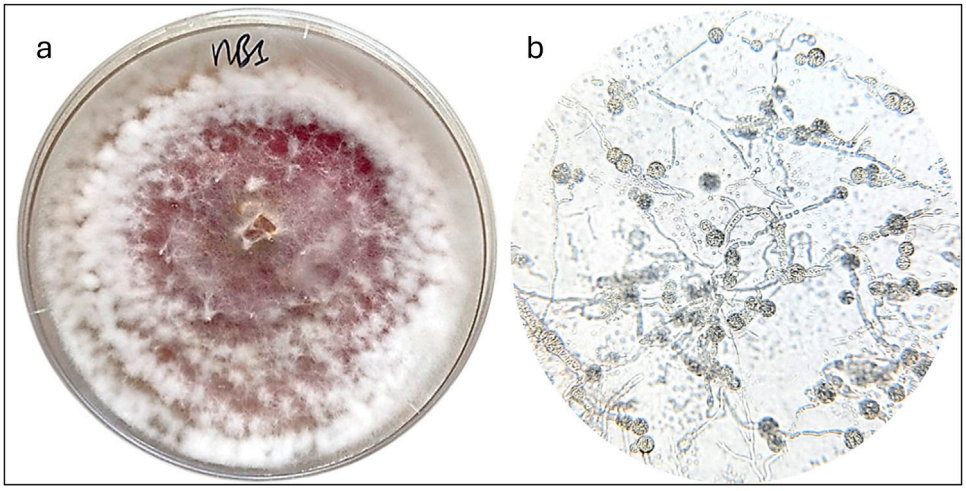

FIGURE 2
Cultural and morphological features of *Fusarium brachygibbosum* **(a)** microscopic view of *Fusarium brachyggibosum* conidia structures observed under compound microscope **(b)** (40X).

3 Results

3.1 Host symptoms and morphological characterization of *Fusarium* strains infecting olive roots

Leaves, roots, and stems were sampled from symptomatic olive trees cultivated in the semi-arid Kairouan region. The olive samples showed typical *Fusarium* infection symptoms, including leaf wilting, chlorosis, and necrosis along the midrib and edges. Stem cross-sections reveal vascular discoloration with brown streaks in the xylem, while roots appear dry, brittle, and necrotic with reduced branching (Figure 1).

Only *Fusarium* strains with white to pink colonies were selected, as the focus is on studying *F. brachygibbosum* species, which are considered emerging pathogens. These strains have recently gained attention due to their characteristic abundant aerial mycelium, aligning with their increasing significance as a plant health threat highlighted by (Bragard et al., 2021).

Colonies grown on PDA reached a diameter of 90 mm at 28°C after 14 days in darkness, characterized by abundant aerial white mycelium, pink colonies (Figure 2a) and rare production of microconidia. Chlamydospores were commonly observed, ranging

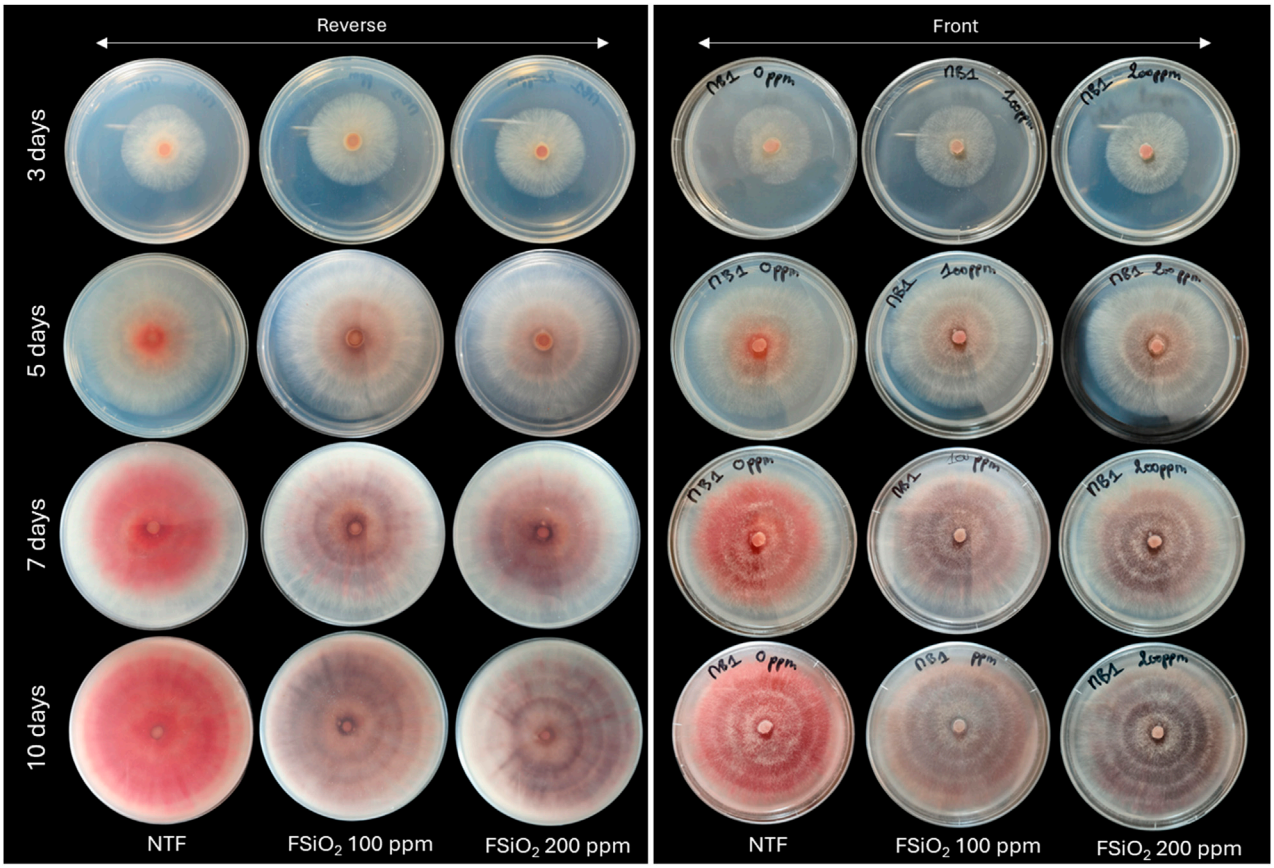

FIGURE 3
Impact of SiO_2 nanoparticles on *Fusarium brachygibbosum* mycelial growth over time on PDA medium: reverse and front views at 100 and 200 ppm compared to the control (NTF).

from 6 to 24 µm in diameter, with a spherical to globose shape, smooth or slightly roughened surfaces, and appearing terminally or intercalarily in chains of two or three (Figure 2b).

Molecular identification at species level was conducted using the internal transcribed spacer (ITS) region of rDNA and the translation elongation factor 1α (TEF-1α). Sequence homology confirmed the identification of the species as *F. brachygibbosum*.

3.2 Inhibitory effects of SiO_2 nanoparticles on *fusarium* growth

The effect of SiO_2 NPs on the fungal growth and structural development of *F. brachygibbosum* was evaluated *in vitro* conditions by using PDA and PDA amended with the compound. Two concentrations of SiO_2 NPs, 100 ppm and 200 ppm, were tested. Observations were conducted after 3, 5, 7, and 10 days of incubation, examining both the reverse and front views of the culture plates. In the control group, *Fusarium* growth exhibited consistent colony expansion and notable red pigmentation, which became more pronounced by day 10. In contrast, *Fusarium* cultured with SiO_2 NPs displayed slower growth and reduced pigmentation, with the inhibitory effect being more evident at the higher concentration of 200 ppm. By day 10, colonies grown with 200 ppm SiO_2 NPs showed smaller diameters and lighter pigmentation compared to both the control and the 100 ppm treatment. These findings suggest a dose-dependent inhibitory effect of SiO_2 nanoparticles on *Fusarium* growth and pigment production, with higher concentrations exerting a greater impact (Figure 3).

To quantify this effect, inhibition rates were measured over time. At 3 dpi, a slight mycelial growth inhibition was observed (3.45% and 1.53% on PDA amended with 100 ppm and 200 ppm, respectively). However, after 3 days, no significant difference was observed ($p < 0.05$) between control and treatments (Table 1). These results indicate that SiO_2 NP could influence fungal colony growth only in the early stages, but their effect diminishes over time. Interestingly, these findings imply that SiO_2 nanoparticles may primarily affect *Fusarium* structural components rather than directly inhibiting mycelium expansion.

Further structural analysis of *F. brachygibbosum* grown under different conditions revealed significant variations (Figure 4). In the control only the fungal hyphae and sparse structures were observed, with no visible macroconidia (Figure 4a). At 100 ppm SiO_2, hyphae and fungal fragments were present, but macroconidia were still absent (Figure 4b). However, treatment with 200 ppm SiO_2 led to the formation of macroconidia, clearly marked by their elongated, canoe-shaped morphology. These observations suggest that while lower concentrations of SiO_2 nanoparticles primarily affect fungal

10.3389/fnano.2025.1569453

TABLE 1 Inhibition rate of growth of Fusarium brachygibbosum grown on PDA medium amended with SiO_2 at concentrations of 100 and 200 ppm, compared to the control group.

Days post-incubation (dpi)	Inhibition rates	
	$FSiO_2$ 100 ppm	$FSiO_2$ 200 ppm
3 dpi (%)	3.45 ± 0.84a	1.53 ± 0.92a
5 dpi (%)	1.34 ± 0.73a	0.22 ± 0.85a
7 dpi (%)	0.19 ± 0.36a	0.4 ± 0.43a
10 dpi (%)	0 a	0 a

Each value represents the mean ± standard error of four replicates per treatment. Means within a line with the same lowercase letter are not significantly different at $p < 0.05$ (Tukey's test). NTF, non treated fusarium; $FSiO_2$ 100 ppm and FSiO2 200 ppm, fusarium treated with 100 and 200 ppm of SiO_2 nanoparticles respectively; dpi, day post incubation.

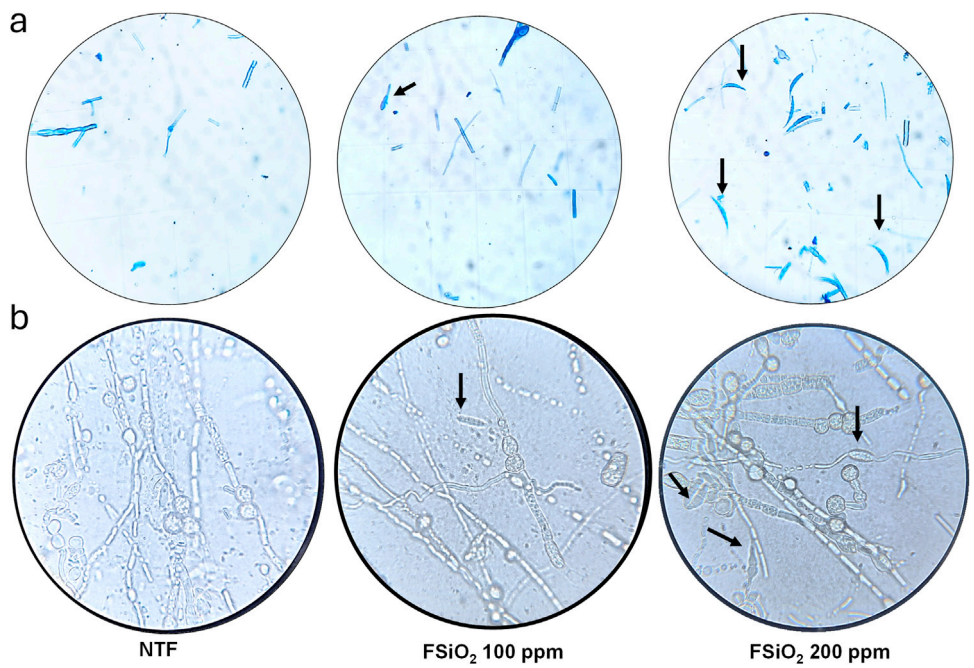

FIGURE 4
Microscopic view of *F. brachyggibosum* conidia structures at 10x **(a)** and 40X **(b)** for.

growth, higher concentrations promote macroconidia formation in *F. brachygibbosum*. This stimulatory effect on macroconidia formation at 200 ppm provides insight into the structural and developmental impacts of SiO_2 nanoparticles on fungal physiology.

The impact of SiO_2 nanoparticles (SiO_2 NPs) on *F. brachygibbosum* spore formation and morphology was assessed by counting the different structures of the fungus. Spore counts revealed clear differences between treatments. Chlamydospore production was highest in the untreated control, while macroconidia were absent in this condition. Treatment with 200 ppm SiO_2 NPs significantly increased the production of macroconidia, whereas the 100 ppm treatment resulted in minimal macroconidia and an intermediate level of chlamydospore production, suggesting a dose-dependent stimulation of macroconidia formation (Figure 5a). The assessment of spore area followed a similar trend. Macroconidia observed in the 200 ppm treatment had the largest area, significantly exceeding those in other treatments. In contrast, the area of chlamydospores remained consistent across the untreated and 100 ppm conditions, indicating a limited effect of lower SiO_2 concentrations on this structural feature (Figure 5b). Furthermore, the perimeter of macroconidia in the 200 ppm treatment was the largest, aligning with the elongated, canoe-shaped morphology noted in previous microscopic observations (Figure 4). Chlamydospores in the untreated and 100 ppm treatments exhibited significantly smaller perimeters, further highlighting the distinct morphological impact of the higher SiO_2 NP concentration (Figure 5c).

These findings align with earlier results, showing that SiO_2 nanoparticles exert a limited effect on mycelial growth but significantly influence *Fusarium* structural development.

3.3 SEM analysis

The analysis of SEM images revealed significant differences in the morphology of *Fusarium* hyphae depending on the concentration of

10.3389/fnano.2025.1569453

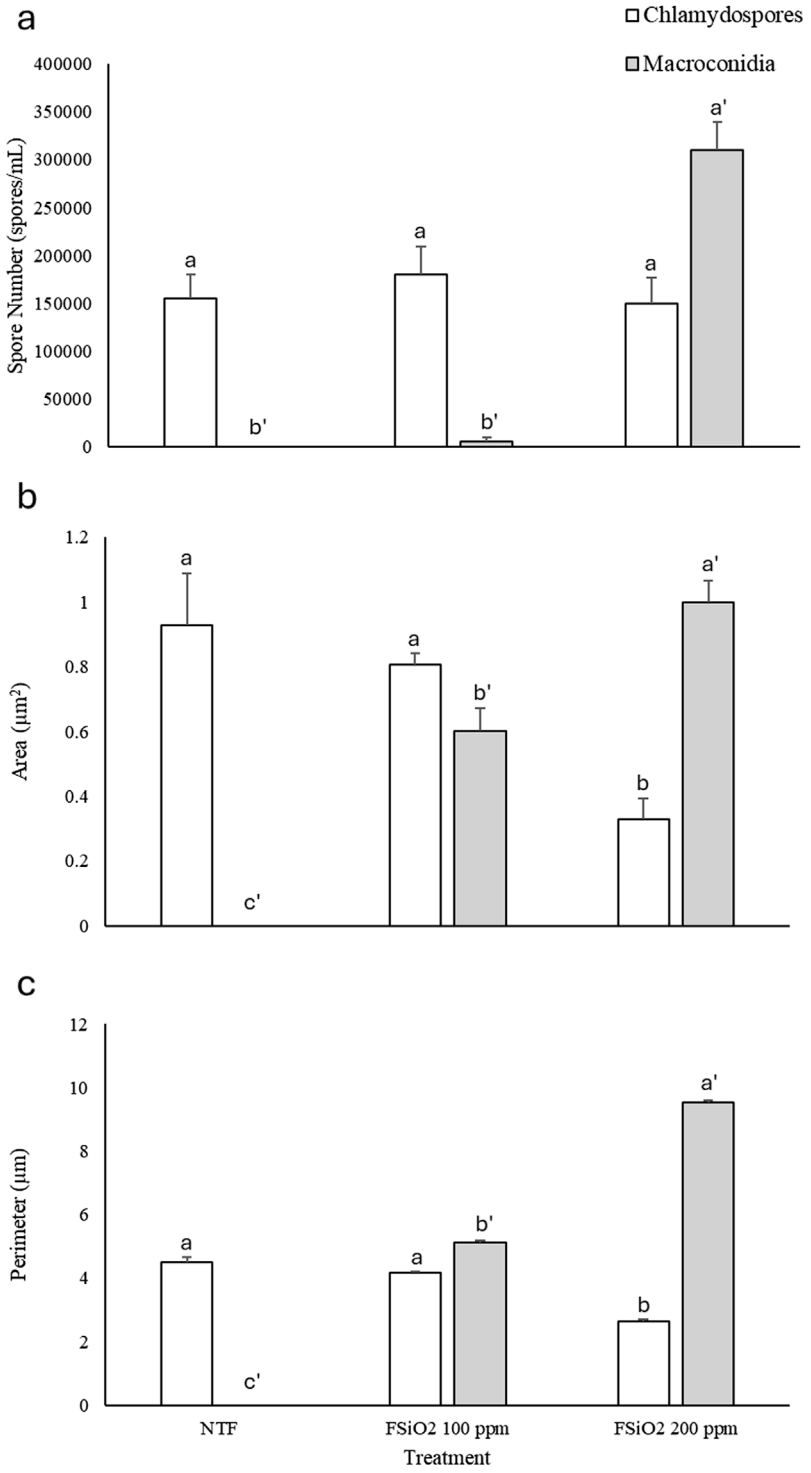

FIGURE 5
Assessement of spore number **(a)** Area **(b)** Perimeter **(c)** of *Fusarium brachygibbosum* spores grown on PDA medium amended with SiO_2 at concentrations of 100 and 200 ppm, compared to the control group. Results represent the mean ± standard error (SE). Bars with a different letter indicate significant differences according to Tukey's HSD test at $P < 0.05$.

SiO_2 nanoparticles and the incubation time. At 3 days post-incubation (dpi), untreated *Fusarium* hyphae exhibited an organized filamentous structure (Figure 6a,d), while the addition of 100 ppm or 200 ppm SiO_2 induced progressive hyphal disorganization, with a more pronounced effect at 200 ppm (Figures 6b,e). At 8 dpi, untreated *Fusarium* showed dense hyphal proliferation, whereas SiO_2 treatments, particularly at 200 ppm, resulted in hyphal fragmentation and an apparent reduction in density.

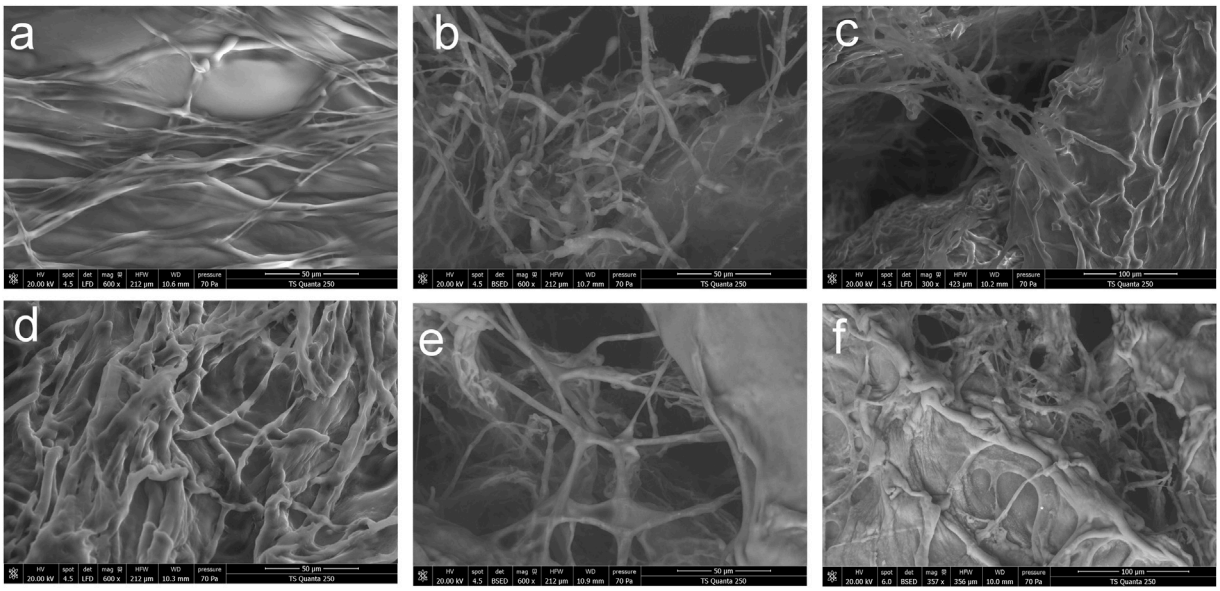

FIGURE 6
Scanning electron micrographs of *Fusarium brachygibbosum* grown on PDA medium amended with SiO_2 at concentrations of 100 and 200 ppm, compared to the control. **(a,d)** Control fungi grown for 3 and 10 days post-incubation (dpi), respectively. **(b,e)**: Fungi grown on PDA medium with 100 ppm SiO_2 for 3 and 10 dpi, respectively. **(c,f)** Fungi grown on PDA medium with 200 ppm SiO_2 for 3 and 10 dpi, respectively.

As a consequence, the assessment of hyphal deformation severity, indicated by mycelium diameter measurement, showed a significant reduction with increasing SiO_2 concentration. The control group exhibited the largest mycelium diameter (7.102 ± 0.463 µm), which was not significantly different from the group treated with 100 ppm SiO_2 (6.151 ± 0.404 µm). However, treatment with 200 ppm SiO_2 resulted in a significantly lower mycelium diameter (3.175 ± 0.158 µm), highlighting the inhibitory effect of higher SiO_2 concentrations on fungal growth (Table 2).

In the SEM micrographs of the treatments with 100 ppm and 200 ppm SiO_2, nanoparticles appeared to be visible on the surface of the hyphae. These particles manifested as small granular structures adhering to the hyphal walls, especially at 200 ppm (Figures 6c,f), where their density seems higher. This suggests direct interaction between the NPs and the hyphae, potentially contributing to the observed inhibitory effect. Such interactions could induce mechanical alterations, modify cell wall permeability, or disrupt normal biological functions of the hyphae.

3.4 Membrane integrity

The mean optical density values obtained at 260 and 280 nm were used to detect absorbing materials, reflecting the potential loss of macromolecules such as nucleic acids and proteins. This loss is associated with plasma membrane disruption and is evident in *F. brachygibbosum* treated with SiO_2 nanoparticles (Table 3). The control group exhibited low optical density values at both wavelengths, indicating intact fungal cells under the given culture conditions. Conversely, treatment with 100 ppm SiO_2 nanoparticles led to a significant rise in the optical density of fungal suspensions, suggesting increased membrane permeability. Surprisingly, the group treated with 200 ppm SiO_2 nanoparticles displayed the lowest absorbance values, a finding that will be further examined in the discussion.

3.5 Impact of SiO_2 on oxidative stress in *Fusarium brachygibbosum*

The impact of SiO_2 supplementation on H_2O_2 content and total antioxidant activity in *Fusarium* spp. was assessed in untreated *Fusarium* (NTF) and cultures grown on PDA supplemented with 100 ppm and 200 ppm SiO_2. The highest H_2O_2 content was recorded in the untreated control, with a significant reduction observed at 100 ppm SiO_2. However, at 200 ppm SiO_2, H_2O_2 levels increased compared to the 100 ppm treatment, though they remained slightly lower than those in the untreated control (Figure 7a). A similar trend was observed for total phenolic compound levels, illustrating the pattern of H_2O_2 variation (Figure 7b).

The total antioxidant activity exhibited a dose-dependent response, with the lowest activity in the untreated control, a moderate increase at 100 ppm SiO_2, and the highest antioxidant activity observed at 200 ppm SiO_2 (Figure 7c).

These results indicate that 100 ppm SiO_2 reduces oxidative stress in *F. brachygibbosum* as evidenced by decreased H_2O_2 levels, while 200 ppm SiO_2 enhances antioxidant activity, potentially as a response to elevated H_2O_2 content.

3.6 Mycotoxin analyses of *Fusarium brachygibbosum* under SiO_2 NPS treatments

The mycotoxin analysis of *F. brachygibbosum* grown on PDA medium amended with SiO_2 nanoparticles (NPs) at concentrations

TABLE 2 Mycelium diameter of *Fusarium brachygibbosum* grown on PDA medium amended with SiO_2 at concentrations of 100 and 200 ppm, compared to the control group.

Treatment	Mycelium diameter (µm)
NTF	7.102 ± 0.463a
$FSiO_2$ 100 ppm	6.151 ± 0.404a
$FSiO_2$ 200 ppm	3.175 ± 0.158b

Each value represents the mean ± standard error of four replicates per treatment. Means within a line with the same lowercase letter are not significantly different at $p < 0.05$ (Tukey's test). NTF, non treated fusarium; $FSiO_2$ 100 ppm and $FSiO_2$ 200 ppm, fusarium treated with 100 and 200 ppm of SiO_2 nanoparticles respectively.

TABLE 3 Detection of absorbing material at 260 and 280 nm in suspensions of *Fusarium brachygibbosum* grown on PDA medium amended with SiO_2 at concentrations of 100 and 200 ppm, compared to the control group.

Treatment	260 nm	280 nm
NTF	1.109 ± 0.006b	0.889 ± 0.001b
$FSiO_2$ 100 ppm	1.533 ± 0.004a	1.213 ± 0.002a
$FSiO_2$ 200 ppm	0.788 ± 0.043c	0.572 ± 0.005c

Each value represents the mean ± standard error of three replicates per treatment. Means within the same column with different letters are significantly different at $p < 0.05$ (Tukey's test). NTF, non treated *fusarium*; $FSiO_2$ 100 ppm and $FSiO_2$ 200 ppm, *fusarium* treated with 100 and 200 ppm of SiO_2 nanoparticles respectively.

of 100 and 200 ppm, compared to the non-treated fungal (NTF) control was able to highlight the change in the quantified mycotoxins including Fusaric Acid (FA), neosolaniol (NEO), 15-acetyldeoxynivalenol (3-15 AC DON), and 4,15-diacetoxyscirpenol (DAS) as represented in Table 4. In the non-treated *Fusarium*, FA was detected at 203.1 mg kg^{-1}, while 3-15 AC DON was present at 57.5 mg kg^{-1}, respectively. NEO and DAS were not detected under these conditions. Upon exposure to 100 ppm SiO_2 NPs, FA remained undetectable, whereas NEO was measured at 1308.4 mg kg^{-1} 3-15 AC DON was produced at a lower concentration (32.4 mg kg^{-1}), while DAS increased to 430.4 mg kg^{-1}. At the higher concentration of 200 ppm SiO_2 NPs, FA remained undetectable, while NEO levels further increased to 2197.3 mg kg^{-1} 3-15 AC DON was not detected in this condition, whereas DAS production rose to 734.2 mg kg^{-1}.

These results indicate that SiO_2 NPs significantly influenced trichothecene biosynthesis in *F. brachygibbosum*, particularly enhancing neosolaniol and DAS production while suppressing FA synthesis. Additionally, 3-15 AC DON levels decreased with increasing SiO_2 NP concentrations, becoming undetectable at 200 ppm.

3.7 *In vitro* assessment of SiO_2 treatment on *fusarium* in olive and sorghum

The effect of SiO_2 NPs at two concentrations (100 and 200 ppm) was assessed on olive tree leaves and stems, and on sorghum shoots. Severe symptoms, including necrosis and browning on leaves and dark streaks or lesions on stems, indicating significant tissue damage, were observed on olive leaves inoculated with untreated *F. brachygibbosum* conidial suspension (Figure 8). Treatment with SiO_2 at 100 ppm reduced these symptoms, with leaves exhibiting milder necrosis and stems showing less browning and lesion formation. At 200 ppm, symptoms were further mitigated, with olive leaves displaying minimal necrosis and stems showing near-normal appearance with reduced streaking.

The measurement of the infected zone rate (%) validates the observed results in Figure 9. The untreated *Fusarium* showed the highest infection severity, with an infected zone rate exceeding 40%, which aligned with the severe necrosis, browning, and tissue damage observed in olive leaves and stems. In contrast, treatments with SiO_2 at 100 ppm and 200 ppm significantly reduce the infected zone rate to approximately 10%. These findings confirm the visual observations, where SiO_2 treatment, particularly at higher concentrations, mitigated symptoms such as necrosis, discoloration, and structural degradation, highlighting its effectiveness in reducing *Fusarium*-induced damage.

For sorghum shoots, the NTF group exhibited extensive tissue degradation and mycelium development. Treatment with SiO_2 at 100 ppm led to moderate recovery, with a reduction in *Fusarium* mycelium development, while at 200 ppm, significant improvement was observed, with shoots showing minimal structural damage and reduced mycelium presence (Figure 8). These results support the observations made on olive trees and confirm the loss of *F. brachygibbosum* pathogenicity under SiO_2 treatment in both olive leaves and shoots and sorghum shoots.

3.8 Analysis of principal components and the relationships among various measured parameters

Based on the principal component analysis (PCA), the first two components, Dim1 (PC1) and Dim2 (PC2), explain 71.8% and 28.2% of the total variance, respectively, providing a comprehensive representation of the dataset's variability (Figure 10). PC1 primarily separates $FSiO_2$ 100 ppm from $FSiO_2$ 200 ppm and NTF, driven by parameters such as H_2O_2 levels, infected zone rate, and fungal growth inhibition. In contrast, PC2 distinctly discriminates $FSiO_2$ 200 ppm from the other samples, with strong contributions from macroconidia-related traits (number, area, and percentage), chlamydospore parameters, and biochemical markers such as polyphenols and AAT

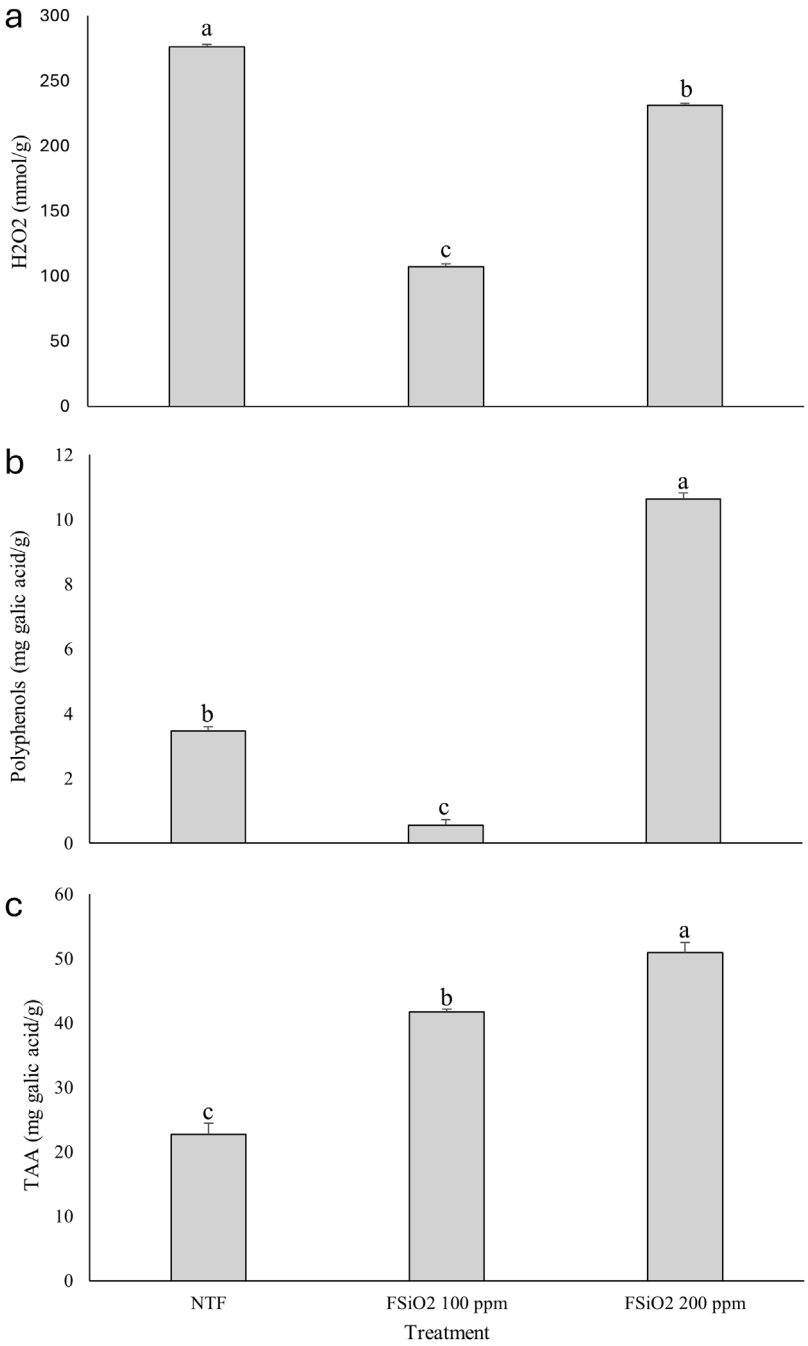

FIGURE 7
Assessment of the peroxyde hydrogen concentration **(a)** total polyphenols concentration **(b)** and total antioxidant activity **(c)** in *Fusarium brachygibbosum* grown on PDA medium amended with SiO_2 at concentrations of 100 and 200 ppm, compared to the control group. Results represent the mean ± standard error (SE). Bars with a different letter indicate significant differences according to Tukey's HSD test at $P < 0.05$.

activity. The PCA highlights a clear dose-dependent effect of $FSiO_2$ nanoparticles on Fusarium physiology and biochemistry, with higher concentrations (200 ppm) inducing more pronounced alterations. The clustering patterns and variable correlations suggest that $FSiO_2$ nanoparticles at higher concentrations effectively disrupt fungal growth and metabolism, with macroconidia and polyphenol-related traits emerging as key indicators of antifungal activity and stress responses.

4 Discussion

Fusarium species have frequently been isolated from olive tissues that display wilt symptoms in Tunisia (Trabelsi et al., 2017) probably due to the co-cultivation of olive trees with other crops susceptible to *Fusarium* infection. Several pathogenic *Fusarium* species were isolated from olive trees showing dieback and wilting symptoms, representing an increasing concern for olive

TABLE 4 Trichothecenes production of *Fusarium brachygibbosum* grown on PDA medium amended with SiO_2 at concentrations of 100 and 200 ppm, compared to the control group.

Treatment	mg/kg mycelium			
	FA	NEO	3-15 AC DON	DAS
NTF	203.1	nd	57.5	nd
$FSiO_2$ 100 ppm	nd	1308.4	32.4	430.4
$FSiO_2$ 200 ppm	nd	2197.3	nd	734.2

FA, Fusaric Acid; NEO, Neosolaniol; 3-15 AC DON, 15-Acetyldeoxynivalenol; DAS, 4,15-Diacetoxyscirpenol; nd, not detected.

producers. Indeed, some *Fusarium* species, including *F. brachygibbosum*, caused important damages in nurseries and newly established olive orchards (Trabelsi et al., 2017). Among the pest management strategies, treatment with synthetic fungicides is the most effective tool against phytopathogenic *Fusarium* species. However, despite the efficacy of chemical pesticides in reducing *Fusarium* growth, their heavy use can lead to the occurrence of resistant strains in the fungal populations (Lucas et al., 2015), as well as adverse environmental impact (Siamak and Zheng, 2018). For that reason, it is crucial to develop alternative eco-friendly tools for controlling *Fusarium* species (Balakumaran et al., 2015). In this study the activity of SiO_2 on *F. brachygybbosum* isolated from olive tree has been evaluated.

4.1 Impact of SiO_2 on mycelium growth and structure

The SiO_2 nanoparticles used in this study exhibit a spherical shape with a uniform and narrow size distribution, as mentioned in our previous work (Baazaoui et al., 2023). Their mesoporous structure and an average particle size of approximately 6 nm contribute to their distinctive physicochemical and morphological properties, which may facilitate effective contact with fungal cells. However, unlike previous studies that reported antifungal activity against Rhizoctonia solani (Abdelrhim et al., 2021), *Alternaria* (Derbalah et al., 2018), and *Fusarium oxysporum* (Parveen and Siddiqui, 2022), their presence did not inhibit mycelial growth. However, SEM analysis revealed significant structural damage to fungal hyphae treated with SiO_2 nanoparticles, including hyphal disorganization, irregular shrinkage, and nanoparticle adherence, particularly at higher concentrations. Similar structural damage was reported for *Fusarium* treated with ZnO or ZnO-CuO nanoparticles, where TEM analysis showed cell wall disintegration, plasma membrane damage, and destruction of intracellular contents (Gaber et al., 2024; Subba et al., 2024). The observed adherence of SiO_2 nanoparticles to the mycelium suggests a direct interaction with the fungal cell wall, potentially affecting its integrity and function. AgNPs have been shown to induce similar effects, forming pits and cavities on the *Fusarium* cell wall, leading to compromised structural integrity and increased permeability (ElSharawy et al., 2023; Todorova et al., 2024). These findings indicate that nanoparticles may disrupt fungal cell wall function, ultimately contributing to oxidative stress and cellular damage.

The harmful effects of nanoparticles on fungal mycelium are further supported by evidence that ions released from nanoparticles penetrate fungal cells, disrupting essential processes such as protein synthesis and DNA replication (Todorova et al., 2024). Our study confirmed these effects, showing DNA damage and loss of plasma membrane integrity when SiO_2 nanoparticles were added at 100 ppm to the *Fusarium* culture medium. However, the absence of effect at 200 ppm could be due to the observed adherence of nanoparticles to the mycelium surface at this concentration. The adherence of nanoparticles to microbial cell membranes, whether through direct or electrostatic interactions, influences membrane permeability (Zhang et al., 2007). This interaction may physically target the membrane, preventing further loss of integrity.

In response to this stress, *F. brachygibbosum* exhibited increased macroconidia sporulation, while chlamydospore production remained unaffected. Asexual spores play a crucial role in fungal survival, enabling colonization of new resource patches, particularly in suboptimal and disturbed environments (Wyatt et al., 2013; Boddy and Hiscox, 2016). Interestingly, stress-induced sporulation has been reported in fungi exposed to resource limitations, where increased investment in spore production allows fungal populations to persist under adverse conditions (Camenzind et al., 2022). Although asexual reproduction is a key factor in the rapid spread of fungal disease outbreaks (Ashu and Xu, 2015), the structural damage induced by SiO_2 NPs may influence the viability or pathogenic potential of the resulting spores, potentially affecting fungal dissemination and host infection dynamics. Given these findings, the increased sporulation observed in *F. brachygibbosum* following SiO_2 treatment may not indicate enhanced fungal proliferation but rather a stress-induced survival mechanism aimed at ensuring persistence under unfavorable conditions. This disruption in fungal cell integrity and function may also contribute to oxidative stress, further exacerbating cellular damage.

4.2 Impact of SiO_2 on fungal oxidative systems and mycotoxin production

SiO_2 nanoparticles demonstrated a concentration-dependent impact on oxidative stress and antioxidant activity in *F. brachygibbosum*. Silicon nanoparticles (SiNPs) have been shown to interact with cellular membranes and induce oxidative stress in various organisms. Specifically, SiO_2 NPs can damage phospholipid

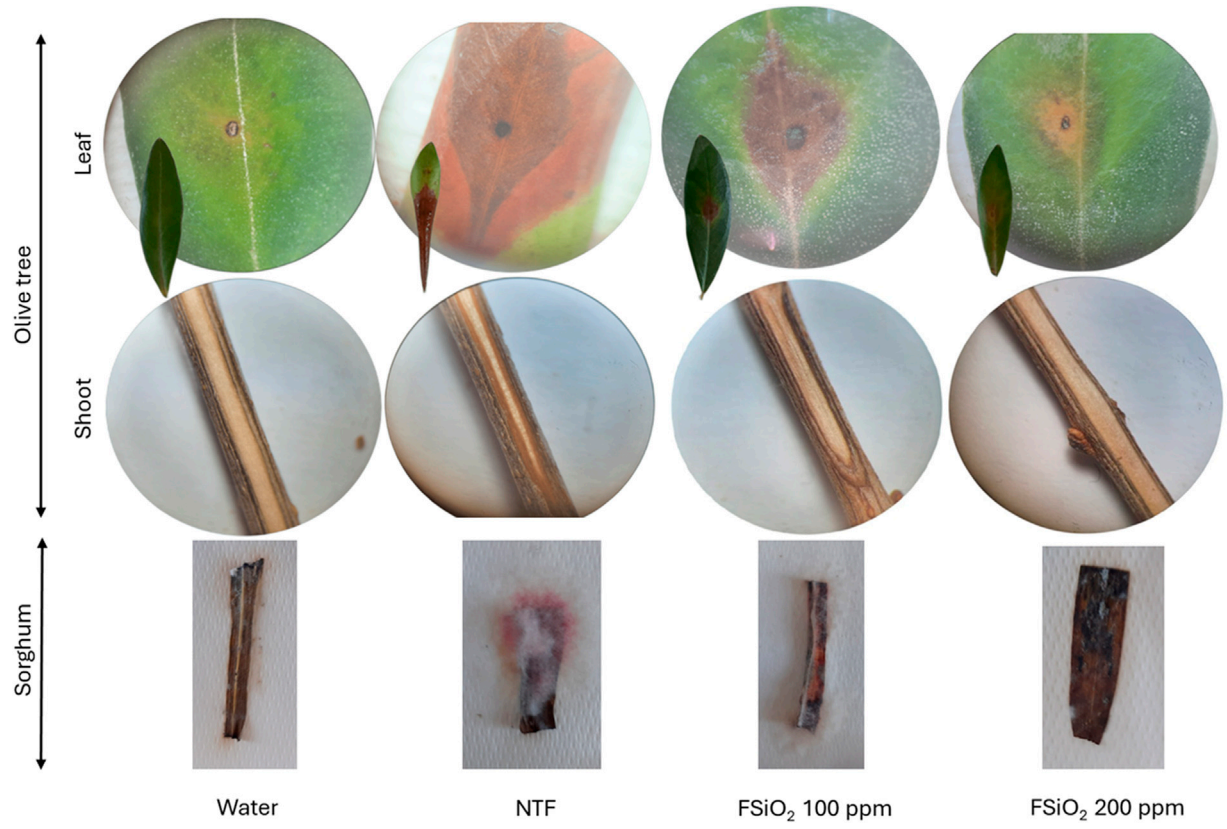

FIGURE 8
Binocular magnifier observations showing symptoms on olive tree leaves and shoots, and sorghum leaves after inoculation with sporal suspensions prepared under different treatments: Water, NTF (untreated), $FSiO_2$ at 100 ppm, and $FSiO_2$ at 200 ppm.

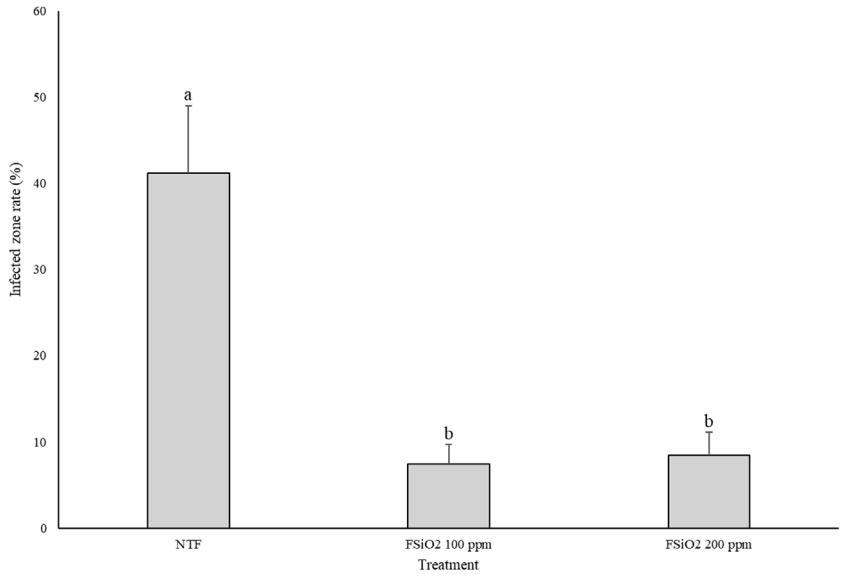

FIGURE 9
Infected surface of olive leaves treated with NTF, $FSiO_2$ 100 ppm and $FSiO_2$ 200 ppm compared to total leaf surface. Results represent the mean ± standard error (SE). Bars with a different letter indicate significant differences according to Tukey's HSD test at $P < 0.05$.

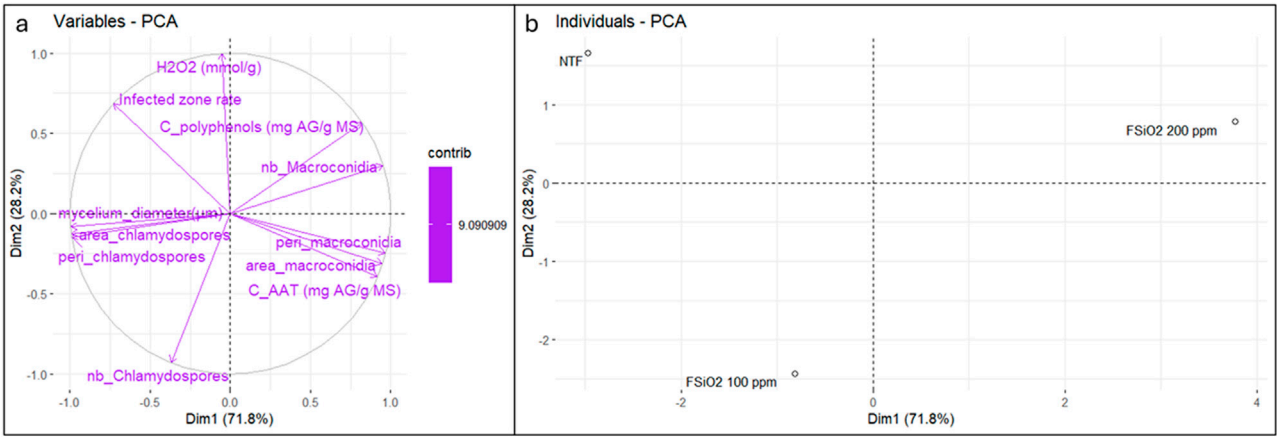

FIGURE 10
Principal component analysis of **(a)** variables influencing the effect of SiO2 nanoparticles on Fusarium brachygibbosum and **(b)** treatments: non-treated fusarium, and fusarium treated with 100 ppm and 200 ppm SiO_2 nanoparticles.

membrane integrity and fluidity, potentially leading to cytotoxicity (Wei et al., 2015). At 100 ppm, SiO_2 significantly reduced oxidative stress by lowering H_2O_2 levels and total polyphenol content, indicating that this concentration effectively mitigates oxidative damage, possibly by enhancing cellular defense mechanisms.

In contrast, at 200 ppm SiO_2, H_2O_2 levels increased compared to the 100 ppm treatment, although they remained lower than those in the untreated group. This suggests that at higher concentrations, SiO_2 exposure may disrupt redox balance, potentially through direct oxidative damage to cellular components. Furthermore, mesoporous silica nanoparticles have been found to induce intracellular peroxidation damage in *Phytophthora infestans* by selectively triggering excess production of reactive oxygen species (ROS), offering potential as a green fungicide for controlling late blight in potatoes (Chen et al., 2023). A similar mechanism may be involved in *F. brachygibbosum*, where the observed increase in total antioxidant activity at 200 ppm suggests an adaptive response to counteract ROS accumulation.

At the proteomic level, previous studies on AgNPs have shown that brief exposure of *E. coli* leads to changes in the expression of envelope proteins (OmpA, OmpC, OmpF, OppA, MetQ) and heat shock proteins (IbpA, IbpB, and ribosomal subunit 30S S6), indicating that the cell membrane is a primary target of nanoparticle-induced stress (Rodrigues et al., 2024). Similarly, SiO_2 NPs may interact with fungal membrane-associated proteins, potentially affecting cell wall integrity and cellular homeostasis. Proteomic analyses of bacteria treated with AgNPs have also revealed elevated levels of antioxidant enzymes such as superoxide dismutase (SOD), catalase (CAT), and peroxidase (POD), along with hydroperoxide resistance proteins, suggesting that oxidative stress plays a central role in nanoparticle toxicity (Liao et al., 2019). Given that SiO_2 NPs induce oxidative stress in *F. brachygibbosum*, a similar proteomic response involving antioxidant defenses may occur in fungi.

The antimicrobial activity of AgNPs has been attributed to a synergistic effect of silver ion release and nanoparticle-specific interactions (Yan et al., 2018). While SiO_2 NPs do not release metal ions in the same manner, their ability to generate ROS and interact with cellular membranes suggests that they may share common cytotoxic mechanisms with AgNPs. However, the precise mode of action of SiO_2 NPs remains unclear. Further studies are needed to elucidate the proteomic changes in fungal cells exposed to SiO_2 NPs, particularly in membrane-associated proteins and oxidative stress response pathways, to better understand their antifungal potential.

Since oxidative stress is known to influence fungal secondary metabolism, these changes in redox balance may also impact the biosynthesis of mycotoxins (Reverberi et al., 2010). Given the observed oxidative stress modulation by SiO_2 nanoparticles, we investigated whether these changes correlated with alterations in trichothecene production by *F. brachygibbosum*.

Our analysis of mycotoxin profiles revealed a distinct pattern dependent on SiO_2 NP concentration. Fusaric acid production was completely inhibited in presence of SiO_2. Previous studies have demonstrated the virulence of this toxin, showing that deletion of key regulatory genes such as *FUB1* and *FUB4* resulted in reduced FA synthesis and decreased virulence of *Fusarium oxysporum* in both plant and mammalian hosts (Ding et al., 2018; López-Díaz et al., 2018). Additionally, FA has been shown to increase host susceptibility to fungal invasion (Liu et al., 2019b), suggesting that its inhibition by SiO_2 NPs could directly impact the pathogenicity of *F. brachygibbosum*. Supporting this, Singh et al. (2017) demonstrated that FA alone can induce Fusarium wilt symptoms in tomato plants, triggering cell death, oxidative stress, and disruptions in photosynthesis and protein expression upon injection of purified FA into tomato leaves.

In contrast to FA, SiO_2 NPs significantly increased NEO production. Previous studies demonstrated that 100 ppm silver nanoparticles reduced NEO production by 9% in *F. chlamydosporum* (Bakri et al., 2020). In our study, the inhibition of FA production under SiO_2 treatments suggests a shift in metabolic flux toward alternative pathways, including NEO biosynthesis (Wei et al., 2022). The absence of FA production could have allowed more precursors to be diverted toward the NEO biosynthesis pathway.

Alternatively, oxidative stress induced by nanoparticles may have influenced mycotoxin biosynthesis in a different way. Ferrigo et al. (2021) reported that H_2O_2 treatment at a lower concentration (1 mM) caused an almost total disappearance of MON and a strong reduction of FBs content in two *Fusarium* species. This suggests that oxidative stress could either suppress specific toxin biosynthesis pathways or trigger compensatory mechanisms leading to increased production of other secondary metabolites. A similar trend was observed with the trichothecene toxin DAS which increased concentration with the increasing dose of nanoparticles. However, 15-Acetyldeoxynivalenol production progressively declined with increasing nanoparticle doses, reaching undetectable levels at highest tested dose.

4.3 Impact of SiO_2 on the reduction of fungal pathogenicity

Patogenicity test revealed a reduced pathogenic effect of *F. brachygibbosum* conidia treated with SiO_2 NPs. Similarly, reduction in H_2O_2 and increasing of total antioxidant activity were observed in *F. brachygibbosum* after treatment. This change in H_2O_2 levels played a significant role in impairing the pathogen's ability to form infection structures necessary for effective host colonization (Scott and Eaton, 2008). ROS, including H_2O_2, are known to act as signaling molecules crucial for fungal differentiation, particularly in the development of structures such as appressoria, which facilitate plant penetration. NADPH oxidases (Nox) are key enzymes responsible for the localized generation of ROS during such processes, and their activity is often essential for fungal virulence (Zhang et al., 2020). Previous studies have demonstrated that fungal mutants with diminished ROS production due to impaired Nox activity exhibit delayed or defective development of primary lesions and a reduction in the functional efficiency of appressoria (Heller and Tudzynski, 2011). This aligns with our observations of reduced necrotic symptoms in leaves inoculated with treated *Fusarium*, suggesting that the treatment may have disrupted the ROS-mediated signaling pathways required for the differentiation of pathogenic structures. This phenomenon is similar to the mode of action of Succinate Dehydrogenase Inhibitor (SDHI) fungicides which impair spore germination by inhibiting succinate dehydrogenase (SDH) (Xu et al., 2019). This disruption prevents the development of infection structures necessary for host colonization, ultimately limiting fungal pathogenicity. Given this similarity, our findings suggest that silicon nanoparticles may have the potential to replace certain conventional pesticides by targeting fungal pathogenicity through comparable mechanisms.

To our knowledge, most studies on the role of SiO_2 NPs in plant-pathogen interactions focused on their ability to enhance plant defense mechanisms (Suriyaprabha et al., 2014; Albalawi et al., 2022; Goswami et al., 2022; Parveen and Siddiqui, 2022). Few *in vitro* studies have been conducted, based only on macroscopic observations rather than molecular analyses (Qin and Tian, 2005). Sakr (2016) demonstrated that the inhibition of *Fusarium* mycelial growth observed in silicon-amended PDA was due to the alkaline pH rather than silicon itself, suggesting that silicon does not have intrinsic antifungal properties. However, the same author hypothesized that the SiO_2 NPs ability to reduce fungal infection severity was due to host-mediated resistance (Sakr, 2021b).

While SiO_2 NPs show potential as nanofertilizers and biopesticides (Sghaier-Hammami et al., 2024), further research is needed to fully understand their long-term impacts on ecosystems and optimize their use in sustainable agriculture (Ahmad et al., 2023). Although SiNPs can potentially enhance soil microbiome and fertility (Rajput et al., 2021; Sghaier-Hammami et al., 2024), there are concerns regarding the accumulation of nanoparticles in soil, which may adversely affect soil microbiota, fertility, and plant growth, as reported by several researchers (Grün et al., 2018; Javed et al., 2019; Baazaoui et al., 2021). An important yet unexplored question is whether fungi can develop resistance to SiO_2 NPs, similar to what has been observed with silver nanoparticles. Studies on silver have shown that fungi can adapt through genetic mechanisms, such as mutations in the *RLM1* gene, which strengthens cell wall integrity, or the activation of copper-transporting ATPases, which help detoxify metal stress (Antsotegi-Uskola et al., 2017; Terzioğlu et al., 2020). Investigating whether similar resistance mechanisms exist for SiO_2 NPs is crucial for assessing their long-term antifungal efficacy and environmental impact. Further research is imperative to better understand the metabolic activity of *F. brachygibbosum* in the presence of SiO_2, not only to explore its fungicidal potential but also to assess its environmental implications. Such inquiries hold the potential to open novel pathways in pesticide research, where silicon could serve not only as a bio-stimulant but also as a fungicide against Fusarium infections in olive trees.

5 Conclusion

This study sheds light on the potential of SiO_2 NPs as a sustainable alternative to conventional fungicides for managing *F. brachygibbosum*, a pathogen threatening olive tree cultivation in Tunisia. Despite SiO_2 NPs not exhibiting direct inhibitory effects on mycelial growth, significant alterations in fungal physiology and mycotoxin production were observed. These findings suggest that SiO_2 NPs interact with the fungus in ways that modify its developmental processes rather than directly inhibiting its growth. Pathogenicity tests further demonstrated that *Fusarium* treated with SiO_2 NPs caused less severe disease symptoms on olive leaves. This reduction in disease severity aligns with the observed changes in fungal sporulation and highlights the ability of SiO_2 NPs to mitigate the pathogen's virulence. The study also revealed that SiO_2 NPs influenced oxidative stress within the fungus, as evidenced by altered H_2O_2 levels and increased antioxidant activity and total polyphenol compounds. The findings underscore the importance of exploring alternative and environmentally friendly strategies to address the challenges posed by *Fusarium* species in agriculture. While this study provides a foundation for using SiO_2 NPs as a tool for fungal management, further research is essential to elucidate their precise mechanisms of action and optimize their application. In particular, comparing their effects with non-nanostructured SiO_2 would help determine whether the observed pathogenicity reductions are specifically due to nanoscale properties. Although the application of nanoparticles in the field, outside of laboratory conditions is still restricted due to the lack of information on the toxicity of these compounds and their impact on the environment,

the preliminary results of this study should encourage research to delve in depth in this aspect to minimize the use of conventional fungicides and limit their deleterious impact.

Data availability statement

The original contributions presented in the study are included in the article, further inquiries can be directed to the corresponding author.

Author contributions

MB: Conceptualization, Writing – original draft, Writing – review and editing, Investigation, Methodology, Validation. BS-H: Conceptualization, Methodology, Project administration, Supervision, Validation, Visualization, Writing – original draft, Writing – review and editing. MM: Investigation, Methodology, Validation, Writing – review and editing. HN: Methodology, Writing – review and editing. SS: Formal Analysis, Methodology, Validation, Writing – review and editing. LG: Methodology, Writing – review and editing. RS: Methodology, Writing – review and editing. MM: Methodology, Writing – review and editing. SL: Investigation, Methodology, Validation, Writing – review and editing. AM: Investigation, Supervision, Writing – review and editing. SBMH: Investigation, Supervision, Validation, Writing – review and editing.

Funding

The author(s) declare that financial support was received for the research and/or publication of this article. This work was supported by the Tunisian Ministry of Higher Education, Scientific Research and Technology under grant number PEJC2023-D4P03.

Acknowledgments

The authors extend their appreciation to the laboratory members for their technical help.

Conflict of interest

The authors declare that the research was conducted in the absence of any commercial or financial relationships that could be construed as a potential conflict of interest.

The author(s) declared that they were an editorial board member of Frontiers, at the time of submission. This had no impact on the peer review process and the final decision.

Generative AI statement

The author(s) declare that no Generative AI was used in the creation of this manuscript.

Publisher's note

All claims expressed in this article are solely those of the authors and do not necessarily represent those of their affiliated organizations, or those of the publisher, the editors and the reviewers. Any product that may be evaluated in this article, or claim that may be made by its manufacturer, is not guaranteed or endorsed by the publisher.

References

Abdelrhim, A. S., Mazrou, Y. S. A., Nehela, Y., Atallah, O. O., El-Ashmony, R. M., Dawood, M. F. A., et al. (2021). Silicon dioxide nanoparticles induce innate immune responses and activate antioxidant machinery in wheat against Rhizoctonia solani. *Plants* 10, 2758. doi:10.3390/plants10122758

Abi Saad, C., Masiello, M., Habib, W., Gerges, E., Sanzani, S. M., Logrieco, A. F., et al. (2022). Diversity of Fusarium species isolated from symptomatic plants belonging to a wide range of agri-food and ornamental crops in Lebanon. *J. Fungi* 8, 897. doi:10.3390/jof8090897

Ahmad, F., Jabeen, K., Iqbal, S., Umar, A., Ameen, F., Gancarz, M., et al. (2023). Influence of silicon nano-particles on Avena sativa L. to alleviate the biotic stress of Rhizoctonia solani. *Sci. Rep.* 13, 15191. doi:10.1038/s41598-023-41699-w

Albalawi, M. A., Abdelaziz, A. M., Attia, M. S., Saied, E., Elganzory, H. H., and Hashem, A. H. (2022). Mycosynthesis of silica nanoparticles using Aspergillus Niger: control of Alternaria solani causing early blight disease, induction of innate immunity and reducing of oxidative stress in eggplant. *Antioxidants* 11, 2323. doi:10.3390/antiox11122323

Al-Hashimi, A., Aina, O., Daniel, A. I., Du Plessis, M., Keyster, M., and Klein, A. (2025). Critical review on characterization, management, and challenges of fusarium head blight disease in wheat. *Physiological Mol. Plant Pathology* 136, 102557. doi:10.1016/j.pmpp.2024.102557

Antsotegi-Uskola, M., Markina-Iñarrairaegui, A., and Ugalde, U. (2017). Copper resistance in Aspergillus nidulans relies on the PI-type ATPase CrpA, regulated by the transcription factor AceA. *Front. Microbiol.* 8, 912. doi:10.3389/fmicb.2017.00912

Ashu, E. E., and Xu, J. (2015). The roles of sexual and asexual reproduction in the origin and dissemination of strains causing fungal infectious disease outbreaks. *Infect. Genet. Evol.* 36, 199–209. doi:10.1016/j.meegid.2015.09.019

Baazaoui, N., Bellili, K., Messaoud, M., Elleuch, L., Elleuch, R., Labidi, S., et al. (2023). Bio-nano-remediation of olive oil mill wastewater using silicon dioxide nanoparticles for its potential use as biofertilizer for young olive plants. *Silicon* 15, 7395–7411. doi:10.1007/s12633-023-02585-2

Baazaoui, N., Sghaier-Hammami, B., Hammami, S. B. M., Khefacha, R., Chaari, S., Elleuch, L., et al. (2021). A handbook guide to better use of nanoparticles in plants. *Commun. Soil Sci. Plant Analysis* 52, 287–321. doi:10.1080/00103624.2020.1836198

Bakri, M. M., El-Naggar, M. A., Helmy, E. A., Ashoor, M. S., and Abdel Ghany, T. M. (2020). Efficacy of juniperus procera constituents with silver nanoparticles against Aspergillus fumigatus and Fusarium chlamydosporum. *BioNanoSci.* 10, 62–72. doi:10.1007/s12668-019-00716-x

Balakumaran, M. D., Ramachandran, R., and Kalaichelvan, P. T. (2015). Exploitation of endophytic fungus, *Guignardia mangiferae* for extracellular synthesis of silver nanoparticles and their *in vitro* biological activities. *Microbiol. Res.* 178, 9–17. doi:10.1016/j.micres.2015.05.009

Bathoova, M., Švubová, R., Bokor, B., Neděla, V., Tihlaříková, E., and Martinka, M. (2021). Silicon triggers sorghum root enzyme activities and inhibits the root cell colonization by *Alternaria alternata*. *Planta* 253, 29. doi:10.1007/s00425-020-03560-6

Bhagat, R., Ingle, A. P., and Chen, H. (2023). "5 - nanosensors and nanobiosensors for sustainable agriculture," in *Nanotechnology in agriculture and agroecosystems*. Editor A. P. Ingle (Elsevier), 93–112. doi:10.1016/B978-0-323-99446-0.00014-3

Boddy, L., and Hiscox, J. (2016). Fungal ecology: principles and mechanisms of colonization and competition by saprotrophic fungi. *Microbiol. Spectr.* 4, doi:10.1128/microbiolspec.funk-0019-2016

Bragard, C., Di Serio, F., Gonthier, P., Jaques Miret, J. A., and Justesen, A. F. (2021). Pest categorisation of Fusarium brachygibbosum. *EFSA J.* 19, e06887. doi:10.2903/j.efsa.2021.6887

Camenzind, T., Weimershaus, P., Lehmann, A., Aguilar-Trigueros, C., and Rillig, M. C. (2022). Soil fungi invest into asexual sporulation under resource scarcity, but trait spaces of individual isolates are unique. *Environ. Microbiol.* 24, 2962–2978. doi:10.1111/1462-2920.16012

Chen, S., Guo, X., Zhang, B., Nie, D., Rao, W., Zhang, D., et al. (2023). Mesoporous silica nanoparticles induce intracellular peroxidation damage of Phytophthora infestans: a new type of green fungicide for late blight control. *Environ. Sci. Technol.* 57, 3980–3989. doi:10.1021/acs.est.2c07182

Chliyeh, M., Msairi, S., Touhami, A. O., Benkirane, R., and Douira, A. (2017). Detection of Fusarium solani as a pathogen causing root rot and wilt diseases of young olive trees in Morocco. *Annu. Res. and Rev. Biol.* 13, 1–7. doi:10.9734/ARRB/2017/33744

Coskun, D., Britto, D. T., Huynh, W. Q., and Kronzucker, H. J. (2016). The role of silicon in higher plants under salinity and drought stress. *Front. Plant Sci.* 7, 1072. doi:10.3389/fpls.2016.01072

Derbalah, A., Shenashen, M., Hamza, A., Mohamed, A., and El Safty, S. (2018). Antifungal activity of fabricated mesoporous silica nanoparticles against early blight of tomato. *Egypt. J. Basic Appl. Sci.* 5, 145–150. doi:10.1016/j.ejbas.2018.05.002

Ding, Z., Yang, L., Wang, G., Guo, L., Liu, L., Wang, J., et al. (2018). Fusaric acid is a virulence factor of Fusarium oxysporum f. sp. cubense on banana plantlets. *Trop. plant Pathol.* 43, 297–305. doi:10.1007/s40858-018-0230-4

Duhan, J. S., Kumar, R., Kumar, N., Kaur, P., Nehra, K., and Duhan, S. (2017). Nanotechnology: the new perspective in precision agriculture. *Biotechnol. Rep.* 15, 11–23. doi:10.1016/j.btre.2017.03.002

El-Abeid, S. E., Ahmed, Y., Daròs, J.-A., and Mohamed, M. A. (2020). Reduced graphene oxide nanosheet-decorated copper oxide nanoparticles: a potent antifungal nanocomposite against Fusarium root rot and wilt diseases of tomato and pepper plants. *Nanomaterials* 10, 1001. doi:10.3390/nano10051001

ElSharawy, A. A., Ibrahim, M. S. S., and Mossa, M. I. (2023). Effect of green biosynthesized silver nanoparticles using Cleome amblyocarpa on controlling chickpea wilt. *Egypt. J. Phytopathology* 51, 1–16. doi:10.21608/ejp.2023.186891.1081

Elsheery, N. I., Helaly, M. N., El-Hoseiny, H. M., and Alam-Eldein, S. M. (2020). Zinc oxide and silicone nanoparticles to improve the resistance mechanism and annual productivity of salt-stressed mango trees. *Agronomy* 10, 558. doi:10.3390/agronomy10040558

Ferrigo, D., Scarpino, V., Vanara, F., Causin, R., Raiola, A., and Blandino, M. (2021). Influence of H2O2-induced oxidative stress on *in vitro* growth and moniliformin and fumonisins accumulation by Fusarium proliferatum and Fusarium subglutinans. *Toxins* 13, 653. doi:10.3390/toxins13090653

Gaber, S. E., Hashem, A. H., El-Sayyad, G. S., and Attia, M. S. (2024). Antifungal activity of myco-synthesized bimetallic ZnO-CuO nanoparticles against fungal plant pathogen Fusarium oxysporum. *Biomass Conv. bioref.* 14, 25395–25409. doi:10.1007/s13399-023-04550-w

Gharbi, Y., Bouazizi, E., Cheffi, M., Ben Amar, F., and Triki, M. A. (2020). Investigation of soil-borne fungi, causal agents of olive trees wilt and dieback in Tunisia. *Archives Phytopathology Plant Prot.* 53, 828–843. doi:10.1080/03235408.2020.1800559

Goswami, P., Sharma, M., Srivastava, N., and Mathur, J. (2022). Assessment of the fungicidal efficacy of biogenic SiO2 NPs in *Eruca sativa* against fusarium wilt. *J. Nat. Pesticide Res.* 2, 100011. doi:10.1016/j.napere.2022.100011

Grün, A.-L., Straskraba, S., Schulz, S., Schloter, M., and Emmerling, C. (2018). Long-term effects of environmentally relevant concentrations of silver nanoparticles on microbial biomass, enzyme activity, and functional genes involved in the nitrogen cycle of loamy soil. *J. Environ. Sci.* 69, 12–22. doi:10.1016/j.jes.2018.04.013

Hassan, I. F., Ajaj, R., Gaballah, M. S., Ogbaga, C. C., Kalaji, H. M., Hatterman-Valenti, H. M., et al. (2022). Foliar application of nano-silicon improves the physiological and biochemical characteristics of 'kalamata' olive subjected to deficit irrigation in a semi-arid climate. *Plants* 11, 1561. doi:10.3390/plants11121561

Heller, J., and Tudzynski, P. (2011). Reactive oxygen species in phytopathogenic fungi: signaling, development, and disease. *Annu. Rev. Phytopathology* 49, 369–390. doi:10.1146/annurev-phyto-072910-095355

Hernández, M. E. S., Dávila, A. R., de Algaba, A. P., López, M. A. B., and Casas, A. T. (1998). Occurrence and etiology of death of young olive trees in southern Spain. *Eur. J. Plant Pathology* 104, 347–357. doi:10.1023/A:1008624929989

Javed, Z., Dashora, K., Mishra, M., D Fasake, V., and Srivastva, A. (2019). Effect of accumulation of nanoparticles in soil health-a concern on future. *Front. Nanosci. Nanotechnol.* 5, 1–9. doi:10.15761/FNN.1000181

Koleva, I. I., Beek, T. A. V., Linssen, J. P. H., Groot, A. D., and Evstatieva, L. N. (2002). Screening of plant extracts for antioxidant activity: a comparative study on three testing methods. *Phytochem. Anal.* 13, 8–17. doi:10.1002/pca.611

Kumari, A., Rana, V., Yadav, S. K., and Kumar, V. (2023). Nanotechnology as a powerful tool in plant sciences: recent developments, challenges and perspectives. *Plant Nano Biol.* 5, 100046. doi:10.1016/j.plana.2023.100046

Leslie, J. F., and Summerell, B. A. (2006). The Fusarium Laboratory Manual. Hoboken: Blackwell Publishing. 1–2. doi:10.1002/9780470278376

Liao, S., Zhang, Y., Pan, X., Zhu, F., Jiang, C., Liu, Q., et al. (2019). Antibacterial activity and mechanism of silver nanoparticles against multidrug-resistant *Pseudomonas aeruginosa*. *Int. J. Nanomedicine* 14, 1469–1487. doi:10.2147/IJN.S191340

Liu, G., Kennedy, R., Greenshields, D. L., Peng, G., Forseille, L., Selvaraj, G., et al. (2007). Detached and attached arabidopsis leaf assays reveal distinctive defense responses against hemibiotrophic colletotrichum spp. *MPMI* 20, 1308–1319. doi:10.1094/MPMI-20-10-1308

Liu, S., Fu, L., Wang, S., Chen, J., Jiang, J., Che, Z., et al. (2019a). Carbendazim resistance of Fusarium graminearum from henan wheat. *Plant Dis.* 103, 2536–2540. doi:10.1094/PDIS-02-19-0391-RE

Liu, S., Li, J., Zhang, Y., Liu, N., Viljoen, A., Mostert, D., et al. (2019b). Fusaric acid instigates the invasion of banana by Fusarium oxysporum f. sp. cubense TR4. *New Phytol.* 225, 913–929. doi:10.1111/nph.16193

López-Díaz, C., Rahjoo, V., Sulyok, M., Ghionna, V., Martín-Vicente, A., Capilla, J., et al. (2018). Fusaric acid contributes to virulence of Fusarium oxysporum on plant and mammalian hosts. *Mol. Plant Pathol.* 19, 440–453. doi:10.1111/mpp.12536

Lucas, J. A., Hawkins, N. J., and Fraaije, B. A. (2015). "Chapter two - the evolution of fungicide resistance," in *Advances in applied microbiology*. Editors S. Sariaslani and G. M. Gadd (Academic Press), 29–92. doi:10.1016/bs.aambs.2014.09.001

Markakis, E. A., Roditakis, E. N., Kalantzakis, G. S., Chatzaki, A., Soultatos, S. K., Stavrakaki, M., et al. (2021). Characterization of fungi associated with olive fruit rot and olive oil degradation in crete, southern Greece. *Plant Dis.* 105, 3623–3635. doi:10.1094/PDIS-10-20-2227-RE

Martínez, J. R., Palomares-Sánchez, S., Ortega-Zarzosa, G., Ruiz, F., and Chumakov, Y. (2006). Rietveld refinement of amorphous SiO2 prepared via sol–gel method. *Mater. Lett.* 60, 3526–3529. doi:10.1016/j.matlet.2006.03.044

Munkvold, G. P., Proctor, R. H., and Moretti, A. (2021). Mycotoxin production in Fusarium according to contemporary species concepts. *Annu. Rev. Phytopathology* 59, 373–402. doi:10.1146/annurev-phyto-020620-102825

Nicoletti, R., Di Vaio, C., and Cirillo, C. (2020). Endophytic fungi of olive tree. *Microorganisms* 8, 1321. doi:10.3390/microorganisms8091321

O'Donnell, K., Kistler, H. C., Cigelnik, E., and Ploetz, R. C. (1998). Multiple evolutionary origins of the fungus causing Panama disease of banana: concordant evidence from nuclear and mitochondrial gene genealogies. *Proc. Natl. Acad. Sci. U. S. A.* 95, 2044–2049. doi:10.1073/pnas.95.5.2044

Parveen, A., and Siddiqui, Z. A. (2022). Impact of silicon dioxide nanoparticles on growth, photosynthetic pigments, proline, activities of defense enzymes and some bacterial and fungal pathogens of tomato. *Vegetos* 35, 83–93. doi:10.1007/s42535-021-00280-4

Pereira, G. A., Arruda, H. S., and Pastore, G. M. (2018). Modification and validation of Folin-Ciocalteu assay for faster and safer analysis of total phenolic content in food samples. *Braz. J. Food Res.* 125, 125. doi:10.3895/rebrapa.v9n1.6062

Qin, G. Z., and Tian, S. P. (2005). Enhancement of biocontrol activity of cryptococcus laurentii by silicon and the possible mechanisms involved. *Phytopathology* 95, 69–75. doi:10.1094/PHYTO-95-0069

Rajput, V. D., Minkina, T., Feizi, M., Kumari, A., Khan, M., Mandzhieva, S., et al. (2021). Effects of silicon and silicon-based nanoparticles on rhizosphere microbiome, plant stress and growth. *Biology* 10, 791. doi:10.3390/biology10080791

Reverberi, M., Ricelli, A., Zjalic, S., Fabbri, A. A., and Fanelli, C. (2010). Natural functions of mycotoxins and control of their biosynthesis in fungi. *Appl. Microbiol. Biotechnol.* 87, 899–911. doi:10.1007/s00253-010-2657-5

Ribeiro, R., Rentes, B. R., Honorato, L. A., and Kuhnen, S. (2024). Effect of nanoemulsion loaded with macela (Achyrocline satureioides) on the ultrastructure of *Staphylococcus aureus* and the modulating activity of antibiotics. *Front. Nanotechnol.* 6, 1466988. doi:10.3389/fnano.2024.1466988

Rodrigues, A. S., Batista, J. G. S., Rodrigues, M. Á. V., Thipe, V. C., Minarini, L. A. R., Lopes, P. S., et al. (2024). Advances in silver nanoparticles: a comprehensive review on their potential as antimicrobial agents and their mechanisms of action elucidated by proteomics. *Front. Microbiol.* 15, 1440065. doi:10.3389/fmicb.2024.1440065

Sakr, N. (2016). The role of silicon (Si) in increasing plant resistance against fungal diseases. *Hellenic Plant Prot. J.* 9, 1–15. doi:10.1515/hppj-2016-0001

Sakr, N. (2021a). pH variation inhibits the mycelial growth of fusarium spp. and cochliobolus sativus. *Pak. J. Phytopathology* 33, 265–273. doi:10.33866/phytopathol.033.02.0637

Sakr, N. (2021b). Soluble silicon controls Fusarium head blight in bread and durum wheat plants. *Gesunde Pflanz.* 73, 479–493. doi:10.1007/s10343-021-00568-0

Sakr, N., and Shoaib, A. (2021). Pathogenic and molecular variation of Fusarium species causing head blight on barley landraces. *Acta Phytopathologica Entomologica Hung.* 56, 5–23. doi:10.1556/038.2021.00006

Santosh, P. S., and Yojana, S. M. (2022). Sustainable management of pesticides. *IJZI 08*, 827–836. doi:10.33745/ijzi.2022.v08i02.100

Scott, B., and Eaton, C. J. (2008). Role of reactive oxygen species in fungal cellular differentiations. *Curr. Opin. Microbiol.* 11, 488–493. doi:10.1016/j.mib.2008.10.008

Sghaier-Hammami, B., Mansour, R. B., Messaoud, M., Baazaoui, N., Ettlili, S., Elleuch, R., et al. (2024). Silicon dioxide (SiO2) nanoparticles as a *Alternaria alternata* fungi mitigator on biomass, photosynthetic machinery, nutriome and antioxidant capacity of barley (hordeum vulgare L.). *Silicon* 16, 4929–4944. doi:10.1007/s12633-024-03031-7

Shahzad, S., Ali, S., Ahmad, R., Ercisli, S., and Anjum, M. A. (2022). Foliar application of silicon enhances growth, flower yield, quality and postharvest Life of tuberose (polianthes tuberosa L.) under saline conditions by improving antioxidant defense mechanism. *Silicon* 14, 1511–1518. doi:10.1007/s12633-021-00974-z

Siamak, S. B., and Zheng, S. (2018). Banana Fusarium wilt (*Fusarium oxysporum* f. sp. *cubense*) control and resistance, in the context of developing wilt-resistant bananas within sustainable production systems. *Hortic. Plant J.* 4, 208–218. doi:10.1016/j.hpj.2018.08.001

Siddiqui, M. H., Al-Whaibi, M. H., Faisal, M., and Al Sahli, A. A. (2014). Nano-silicon dioxide mitigates the adverse effects of salt stress on Cucurbita pepo L. *Environ. Toxicol. Chem.* 33, 2429–2437. doi:10.1002/etc.2697

Singh, V. K., Singh, H. B., and Upadhyay, R. S. (2017). Role of fusaric acid in the development of '*Fusarium* wilt' symptoms in tomato: physiological, biochemical and proteomic perspectives. *Plant Physiology Biochem.* 118, 320–332. doi:10.1016/j.plaphy.2017.06.028

Subba, B., Rai, G. B., Bhandary, R., Parajuli, P., Thapa, N., Kandel, D. R., et al. (2024). Antifungal activity of zinc oxide nanoparticles (ZnO NPs) on *Fusarium equiseti* phytopathogen isolated from tomato plant in Nepal. *Heliyon* 10, e40198. doi:10.1016/j.heliyon.2024.e40198

Suriyaprabha, R., Karunakaran, G., Kavitha, K., Yuvakkumar, R., Rajendran, V., and Kannan, N. (2014). Application of silica nanoparticles in maize to enhance fungal resistance. *IET Nanobiotechnology* 8, 133–137. doi:10.1049/iet-nbt.2013.0004

Terzioğlu, E., Alkım, C., Arslan, M., Balaban, B. G., Holyavkin, C., Kısakesen, H. İ., et al. (2020). Genomic, transcriptomic and physiological analyses of silver-resistant *Saccharomyces cerevisiae* obtained by evolutionary engineering. *Yeast* 37, 413–426. doi:10.1002/yea.3514

Todorova, D., Yavorov, N., and Vrabič-Brodnjak, U. (2024). Impact of silver nanoparticle treatment and chitosan on packaging paper's barrier effectiveness. *Polymers* 16, 2127. doi:10.3390/polym16152127

Trabelsi, R., Sellami, H., Gharbi, Y., Krid, S., Cheffi, M., Kammoun, S., et al. (2017). Morphological and molecular characterization of Fusarium spp. associated with olive trees dieback in Tunisia. *3 Biotech.* 7, 28. doi:10.1007/s13205-016-0587-3

Velikova, V., Yordanov, I., and Edreva, A. (2000). Oxidative stress and some antioxidant systems in acid rain-treated bean plants: protective role of exogenous polyamines. *Plant Sci.* 151, 59–66. doi:10.1016/S0168-9452(99)00197-1

Verma, R., Kushwaha, K. P. S., Kumar, S., Rawat, S., Pandey, R., Pandey, D., et al. (2024). Emerging threat to Indian agriculture: *Fusarium incarnatum-equiseti* species complex as a novel pathogen imperiling bajra, cowpea, finger millet, green gram, moth bean, and soybean crops. *Crop Prot.* 182, 106741. doi:10.1016/j.cropro.2024.106741

Wei, X., Jiang, W., Yu, J., Ding, L., Hu, J., and Jiang, G. (2015). Effects of SiO2 nanoparticles on phospholipid membrane integrity and fluidity. *J. Hazard. Mater.* 287, 217–224. doi:10.1016/j.jhazmat.2015.01.063

Wei, X., Wang, W.-G., and Matsuda, Y. (2022). Branching and converging pathways in fungal natural product biosynthesis. *Fungal Biol. Biotechnol.* 9, 6. doi:10.1186/s40694-022-00135-w

Wyatt, T. T., Wösten, H. A. B., and Dijksterhuis, J. (2013). "Chapter two - fungal spores for dispersion in space and time," in *Advances in applied microbiology*. Editors S. Sariaslani and G. M. Gadd (Academic Press), 43–91. doi:10.1016/B978-0-12-407672-3.00002-2

Xu, C., Li, M., Zhou, Z., Li, J., Chen, D., Duan, Y., et al. (2019). Impact of five succinate dehydrogenase inhibitors on DON biosynthesis of Fusarium asiaticum, causing Fusarium head blight in wheat. *Toxins* 11, 272. doi:10.3390/toxins11050272

Yan, X., He, B., Liu, L., Qu, G., Shi, J., Hu, L., et al. (2018). Antibacterial mechanism of silver nanoparticles in *Pseudomonas aeruginosa*: proteomics approach. *Metallomics* 10, 557–564. doi:10.1039/c7mt00328e

Yin, Y., Liu, X., Li, B., and Ma, Z. (2009). Characterization of sterol demethylation inhibitor-resistant isolates of Fusarium asiaticum and F. Graminearum collected from wheat in China. *Phytopathology®* 99, 487–497. doi:10.1094/PHYTO-99-5-0487

Yobo, K. S., Mngadi, Z. N. C., and Laing, M. D. (2019). Efficacy of two potassium silicate formulations and two trichoderma strains on Fusarium head blight of wheat. *Proc. Natl. Acad. Sci. India, Sect. B Biol. Sci.* 89, 185–190. doi:10.1007/s40011-017-0935-z

Yuan, S., and Zhou, M. (2005). A major gene for resistance to carbendazim, in field isolates of *Gibberella zeae*. *Can. J. Plant Pathology* 27, 58–63. doi:10.1080/07060660509507194

Zhang, L., Jiang, Y., Ding, Y., Povey, M., and York, D. (2007). Investigation into the antibacterial behaviour of suspensions of ZnO nanoparticles (ZnO nanofluids). *J. Nanopart Res.* 9, 479–489. doi:10.1007/s11051-006-9150-1

Zhang, Z., Chen, Y., Li, B., Chen, T., and Tian, S. (2020). Reactive oxygen species: a generalist in regulating development and pathogenicity of phytopathogenic fungi. *Comput. Struct. Biotechnol. J.* 18, 3344–3349. doi:10.1016/j.csbj.2020.10.024

Ziaee, M., and Ganji, Z. (2016). Insecticidal efficacy of silica nanoparticles against Rhyzopertha Dominica F. and *Tribolium confusum* Jacquelin du Val. *J. Plant Prot. Res.* 56, 250–256. doi:10.1515/jppr-2016-0037